PHYSICAL REVIEW C VOLUME 7, NUMBER 2 FEBRUARY 1973

Pauli Exclusion Effects in Reactions Involving Multinucleon Systems*

B. L. Gambhir
Department of Physics and Astronomy, University of Rochester, Rochester, New York 14627

and

James J. Griffin†
Lawrence Berkeley Laboratory, Nuclear Chemistry Division, Berkeley, California 94720

(Received 6 November 1972)

To investigate the importance of effects of Pauli exclusion principle in reactions involving multinucleon systems, we consider reactions in which deuterons are incident on a recoilless nucleus. First, the binding energy of a model deuteron in the presence of a nuclear Fermi gas (an infinite nucleus) is calculated as a function of nuclear density and deuteron kinetic energy so as to provide some clues to the range of incident energies and nuclear densities where exclusion effects can be expected to be important. The results show that this model deuteron is unbound in the presence of infinite nuclear matter, unless it has a kinetic energy, at least, of the order of 100 MeV. Making some simplifying assumptions, then, we pose a model problem and obtain for the deuteron breakup, elastic scattering, and stripping reactions, Hilbert-Schmidt integral equations in which the Pauli term, in each case, can be identified. Corresponding to Pauli breakup term, Pauli breakup cross sections for deuterons on ^{16}O nucleus have been calculated in a simple model. The dependence of cross sections on directions along which the breakup products emerge and the energy partition among them is investigated. The variation of cross section with incident deuterons' kinetic energy and with nuclear density is also studied. The most prominent and important feature of Pauli breakup is the sharp peaking of cross sections for very asymmetric partition of energy among outgoing particles and is very encouraging for an experimental test. Finally, by considering Pauli breakup of an artifically tightly bound deuteron, we conclude that the Pauli mechanism should be of importance in α-particle reactions as well.

I. INTRODUCTION

A. Exclusion Effects in Nuclear Reactions Involving Multinucleon Projectiles and Targets

The dominant role played by the Pauli exclusion principle in atomic collisions involving multielectron atoms has been recognized for several years.[1] Recently Brandt and Laubert[2] have reported data on cross sections for the ionization of K shells of Al in collisions with swift heavy atoms. In comparison with Coulomb-excitation cross sections, the cross sections observed by them are enormous – some 10^3 to 10^5 times larger. They attribute the large cross sections to the exchange forces set up during collisions by the Pauli exclusion principle in the overlapping electron clouds of the interpenetrating atoms. The analogous Pauli mechanism, so far, has not received much consideration in nuclear reactions involving multinucleon bound projectiles and targets. The importance of Pauli exclusion principle in these reactions has been recognized by several authors[3-9] but no explicit calculation exists which takes into account the influence of Pauli exclusion principle on the projectile as it passes through the region occupied by the target.

The work of Junkin and Villars[8] is of special interest to us as it deals with deuteron reactions. It gives a formally complete treatment of the deuteron breakup problem. However, the influence of Pauli exclusion principle cannot be seen explicitly in their formal results, nor are the results amenable to numerical estimates.

Baumgärtner[10] has estimated the influence of Pauli exclusion principle on the optical model for elastic deuteron scattering in an infinite-nuclear-matter approximation and finds the effect to be small. However, it may be misleading to generalize this conclusion to the case of finite nuclei as Thouless[9] has shown in another context that the finite size of the nucleus and curvature of nuclear surface must be taken into account from the beginning for a complete description of nuclear reactions.

Recently Johnson and Soper[11] have also mentioned the possible corrections to the deuteron elastic and stripping reactions arising from the considerations of Pauli exclusion principle.

B. Outline of Presentation

In this paper we describe the deuteron breakup on a recoilless nucleus as the simplest prototype of reactions involving multinucleon systems. Our treatment includes the "Pauli exclusion" effects of antisymmetrization but neglects certain exchange effects by treating the nucleons in the deuteron as identical to, but distinguishable from, nucleons in the nucleus, i.e., it is more in the spirit of a Hartree rather than a Hartree-Fock calculation. Then, a model problem is defined and preliminary inferences regarding the implications of exclusion effects are drawn.[12] Some possible applications and extensions of the basic formalism are also discussed.

Section II illustrates the mechanism by which the Pauli exclusion principle can cause deuteron breakup. In Sec. III we discuss the bound state of the deuteron. We also study the variation of its binding energy inside nulcear matter due to exclusion principle restrictions as a function of both the center-of-mass momentum K_0 and the Fermi momentum k_f. Thereby we get clues to the range of incident energies and nuclear densities where the Pauli exclusion principle may be an important mechanism in deuteron reactions.

In Sec. IV we describe our model deuteron nucleus scattering problem. In Sec. V we obtain a well-behaved integral equation for the breakup amplitude, and identify the Pauli breakup amplitude. Section VI obtains similar integral equations for deuteron elastic scattering and stripping reactions. Section VII is devoted towards obtaining an approximate formula for Pauli breakup cross section on which the numerical calculations are based. The numerical results are discussed in Sec. VIII, in particular the dependence of cross sections on:
(1) the directions along which breakup products emerge;
(2) the partition of energy among the outgoing neutron and proton;
(3) incident deuteron's kinetic energy;
(4) the nuclear density;
(5) compatible sets of deuteron parameters, discussed in some detail.

Finally, by considering the Pauli breakup of an artificially tightly bound deuteron, qualitative inferences regarding the importance of Pauli mechanism in α-particle reactions are drawn (Sec. IX).

II. OVERVIEW OF THE PHYSICS OF PAULI EXCLUSION PRINCIPLE

In this section we describe the mechanism by which the Pauli exclusion principle can cause deuteron breakup. Consider a deuteron propagating through free space with a momentum K_0. Its complete wave function may be expanded in plane-wave products, i.e.,

$$\phi_0(\vec{r})e^{i\vec{K}_0\cdot\vec{R}} = \int \phi_0(\vec{k})e^{i\vec{k}_+\cdot\vec{r}_+}e^{i\vec{k}_-\cdot\vec{r}_-}d^3k, \qquad (2.1)$$

where $\vec{k}_\pm = \frac{1}{2}\vec{K}_0 \pm \vec{k}$ and $\vec{r}_\pm = \vec{R} \pm \frac{1}{2}\vec{r}$.

Next consider the deuteron to be propagating through infinite nuclear matter with the same momentum K_0. Let us assume that infinite nuclear matter can be described adequately by the Fermi-gas model; i.e., all plane-wave states with momentum less than or equal to the Fermi momentum, k_f, are filled and all other states are empty. Then on account of the Pauli exclusion principle those plane-wave products in Eq. (2.1) which correspond to either k_+ or k_- less than k_f will be for-

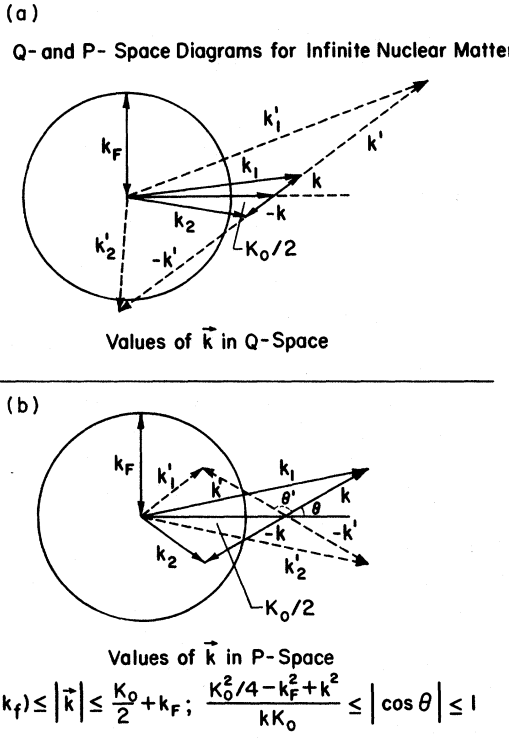

FIG. 1. Illustration of the operators $Q(K_0, k_f)$ and $P(K_0, k_f)$, where K_0=deuteron center-of-mass momentum, k_f=Fermi momentum of the nuclear Fermi gas through which the deuteron is propagating. The value of K_0 is considered to be greater than $2k_f$. Part (a) illustrates two values $(\vec{k}, \vec{k}')$ of the neutron-proton relative momentum which are allowed, i.e., are in Q space. One of these is smaller than $\frac{1}{2}K_0 - k_f$, while the other, k', is greater than $\frac{1}{2}K_0 + k_f$. Similarly part (b) shows two possible values $(\vec{k}, \vec{k}')$ of the neutron-proton relative momentum that are in P space; $P = 1 - Q$. The expression at the bottom of this figure sums up the extent of the P space for the case of K_0 greater than $2k_f$.

bidden for the deuteron. In other words some of the relative momenta are not allowed. We shall refer to the forbidden part of the phase space as P space and the allowed part as the Q space. Figure 1 shows two examples in each case of relative momenta belonging to Q space and P space, respectively, while the equation

$$|\tfrac{1}{2}K_0 - k_f| < |\vec{k}| < \tfrac{1}{2}K_0 + k_f ;$$
$$\frac{\frac{1}{4}K_0^2 - k_f^2 + k^2}{kK_0} < |\cos\theta| < 1 , \quad \cos\theta = (\hat{K}_0 \cdot \hat{k}) \qquad (2.2)$$

sums up the extent of P space for the case of $K_0 > 2k_f$. These phase-space restrictions on the internal motion of the deuteron result in its distortion into a new modified state. This modified state will have definite nonvanishing overlap with the free space bound state of the deuteron as well as its unbound states. As a result the Pauli mechanism can contribute directly to the deuteron elastic scattering and breakup reactions and through coupling influences the deuteron stripping reactions as well.

III. BOUND STATE OF DEUTERON

Some insight into the role of Pauli mechanism in deuteron reactions can be obtained by considering its effect on the bound state of the deuteron. We derive, in a simple model, an expression for the binding energy of a deuteron propagating with center-of-mass momentum K_0, through an infinite nuclear Fermi gas with Fermi momentum k_f. We study the variation of this binding energy as a function of both K_0 and k_f. Thereby we get clues to the range of incident energies and nuclear densities where Pauli mechanism can be expected to be important in deuteron reactions.

Since we are interested in qualitative or semiquantitative understanding of a little-studied phenomenon, our simple model for the deuteron assumes the neutron-proton interaction to be given by a Yamaguchi[13] type one-term separable potential

$$V_{np}(k|k') = -f(k)f(k'); \quad f(k) = g/(k^2 + a^2) , \qquad (3.1)$$

thus allowing us to obtain analytic expressions in many places and keep the discussion transparent and simple. The parameters a, g of this potential were chosen to fit the binding energy ϵ_0 and mean square radius $\langle r^2 \rangle$ of the deuteron. Details of this parameter fit are discussed in Appendix A.

A. Deuteron in Free Space

For the purpose of the present work it is advantageous to work in the momentum representation. Since V_{np} does not depend on the center-of-mass coordinates (translational invariance), we can write for the complete wave function $\psi_0(K, k) = \delta^3(\vec{K} - \vec{K}_0)\phi_0(k)$, with $\phi_0(k)$ satisfying the Schrödinger equation for relative motion,

$$k^2\phi_0(k) + \int V_{np}(k|k')\phi_0(k')d^3k' = -k_0^2\phi_0(k) , \qquad (3.2)$$

where $k_0^2 = \epsilon_0$ is the deuteron binding energy. Here, and in the rest of this paper, we use units such that $\hbar = M = 1$, where M is the nucleon mass. Then dimensions of energy are those of (inverse length),[2] and the conversion factor is 1 fm^{-2} = 41.5 MeV.

Substituting for V_{np} from Eq. (3.1) into Eq. (3.2), one gets the result

$$\phi_0(k) = cf(k)/(k^2 + k_0^2) , \qquad (3.3)$$

where

$$c = \int f(k')\phi_0(k')d^3k' . \qquad (3.4)$$

On substituting from Eq. (3.3) into Eq. (3.4) one gets the eigenvalue equation

$$1 = \int d^3k |f(k)|^2/(k^2 + k_0^2) = \frac{\pi^2 g^2}{a(a + k_0)^2} . \qquad (3.5)$$

However, we shall adopt for k_0^2 the experimentally known value of deuteron binding energy which in our units is 0.053 64 fm^{-2} (2.226 MeV) and consider Eq. (3.5) to be a condition on the parameters of the potential V_{np}.

Next, we proceed to discuss modifications to these equations which arise from considerations of Pauli exclusion principle when the deuteron is propagating through infinite nuclear matter.

B. Deuteron in Infinite Nuclear Matter: Effects of Pauli Exclusion Principle

Some results on the variation of the binding energy of a deuteron propagating through infinite nuclear matter have already been reported.[14,15] For the description of the deuteron, Refs. 14 and 15 use separable potential models similar to the one used here. We shall report here only the calculations for the case of center-of-mass momentum $K_0 > 2k_f$, where k_f is the Fermi momentum.[16] The reason for this is as follows. We are interested in nuclear reactions where the incident deuterons have positive kinetic energy. On entering nuclear matter these deuterons will travel with a center-of-mass momentum[17] $K_0 > 2k_f$.

When the deuteron is propagating through infinite nuclear matter, the translational invariance argument still holds, and therefore we have $\bar{\psi}_0(\vec{K}, \vec{k}) = \delta^3(\vec{K} - \vec{K}_0)\bar{\phi}_0(k)$. The wave function $\bar{\phi}_0(k)$, therefore, satisfies the same equation as $\phi_0(k)$, i.e.,

Eq. (3.2). However, due to Pauli exclusion principle, $\bar{\phi}_0(k)$ is nonzero only when $\vec{k}$ is such that both $|\vec{K}_0+\vec{k}|$ and $|\vec{K}_0-\vec{k}|$ are greater than k_f, i.e., when $\vec{k}$ belongs to Q space (see Sec. II and Fig. 1). The net result of this boundary condition is that the effective interaction becomes

$$\bar{V}_{np}(k|k') = -\bar{f}(k)\bar{f}(k'), \tag{3.6}$$

where

$$\bar{f}(k) = f(k) \quad \text{when } \vec{k} \text{ is } Q \text{ space},$$
$$= 0 \quad \text{when } \vec{k} \text{ is } P \text{ space}. \tag{3.7}$$

We therefore get a different eigenvalue, $\bar{\epsilon}_0 = \bar{k}_0^2$, given by the following equation:

$$1 = \int d^3k \bar{f}(k)^2/(k^2+\bar{k}_0^2) = \int_{Q\text{ space}} d^3k f(k)^2/(k^2+\bar{k}_0^2). \tag{3.8}$$

Comparing this equation with Eq. (3.5), it is obvious that since the integrand is positive definite over the whole range, the restricted space implies $\bar{k}_0 < k_0$.

The integral in Eq. (3.8) can be carried out exactly giving the result

$$1 = \frac{\pi^2 g^2}{a(a+\bar{k}_0)^2} - I_0(K_0, k_f, \bar{k}_0), \tag{3.9}$$

where I_0 is given by

$$I_0 = \frac{4\pi g}{(a^2-\bar{k}_0^2)^2}\left[\frac{\bar{k}_0^2 - AB}{2K_0}\ln\left(\frac{A^2+\bar{k}_0^2}{B^2+\bar{k}_0^2}\,\frac{B^2+a^2}{A^2+a^2}\right) + \frac{a^2+\bar{k}_0^2}{2a}\tan^{-1}\frac{2k_f a}{a^2+AB} - \bar{k}_0\tan^{-1}\frac{2k_f\bar{k}_0}{\bar{k}_0^2+AB}\right], \tag{3.10}$$

where $A = \frac{1}{2}K_0 + k_f$ and $B = \frac{1}{2}K_0 - k_f$. An interesting limiting value of I_0 arises for the case of $K_0 \gg k_f, a, k_0$:

$$I_0 \simeq \frac{128 g^2}{K_0^3}\,\frac{4}{3}\,\pi\,\frac{k_f^3}{K_0^3}\left|1 + \frac{4(3k_f^2 - 2a^2 - \bar{k}_0^2)}{K_0^2}\right|, \tag{3.11}$$

$$K_0 \gg k_f, a, \bar{k}_0.$$

Thus in the high-energy limit the correction term

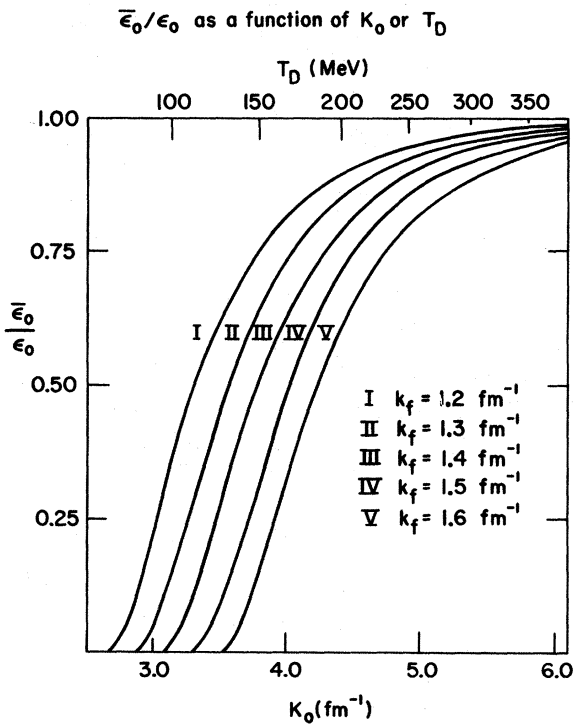

FIG. 2. The variation of binding energy $\bar{\epsilon}_0$ (considered a positive quantity) with center-of-mass momentum for a deuteron propagating through a nuclear Fermi gas (Fermi momentum $= k_f$) is shown for a few different values of k_f. $\bar{\epsilon}_0$ is measured in units of free space deuteron binding energy, ϵ_0.

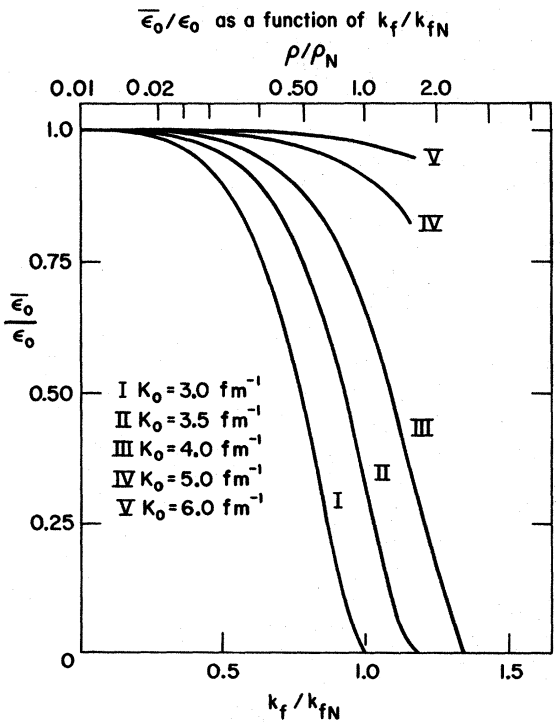

FIG. 3. The curves in this figure illustrate the variation of $\bar{\epsilon}_0/\epsilon_0$ as a function of ρ and k_f [$\rho = (2/3\pi^2)k_f^3$]. ρ is measured in units of nuclear matter density, i.e., 0.17 nucleons/fm^3, while k_f is measured in units of corresponding Fermi momentum $k_{fN} = 1.36$ fm^{-1}.

in the energy eigenvalue Eq. (3.9) as compared to Eq. (3.5) is linearly proportional to the volume of Fermi sphere or the density of nuclear matter and inversely proportional to the cube of deuteron kinetic energy.

The solution to Eq. (3.9) for different values of K_0, k_f is depicted in Figs. 2 and 3.

C. Inferences About the Importance of Pauli Mechanism in Deuteron Reaction from Variation of Binding Energy with K_0, k_f

One may consider a large but finite nucleus to be infinite nuclear matter of varying density.[18] Then the result of Figs. 2 and 3 may be used to infer the range of incident energies and parts of the nuclear region which are of importance in Pauli breakup. The steep rise of the curves in Fig. 2 suggests that the Pauli breakup cross sections will drop very rapidly with increasing incident energy. Similarly Fig. 3 suggests that the contribution to Pauli breakup from the low-density nuclear tail will be small.

In order to make the above-mentioned qualitative remarks a little more specific, let us assume that the circumstances for which the curves in Figs. 2 and 3 predict a 10% or more difference between the deuteron binding energies in nuclear matter and in free space, one would expect the Pauli mechanism to play an important role. Then in Fig. 2, curve II,[19] $\bar{\epsilon}_0/\epsilon_0 = 0.90$ at $K_0 = 4.71$ fm^{-1} or $T_d = 230$ MeV.

In these figures K_0, T_d refer to the deuteron center-of-mass momentum and kinetic energy, respectively, when propagating inside the nuclear matter. If the increase in kinetic energy of the deuteron on entering nuclear matter is 80 MeV (reasonable number on the basis of what is known about nucleon-nucleus optical potentials). Then $T_d = 230$ MeV corresponds to an incident deuteron kinetic energy, $E_d = 150$ MeV. Thus for incident energy E_d up to 150 MeV one can expect the Pauli breakup cross sections to be significant.

Using the same criterion, from Fig. 3, we find that for $K_0 = 4.0$ fm^{-1} ($E_d \simeq 76$ MeV) the region of the nucleus where density is greater than $0.44\rho_N$ (ρ_N is the equilibrium nuclear matter density = 0.17 nucleons/fm^3 and corresponds to $k_{fN} = 1.36$ fm^{-1}) will be important in Pauli breakup. Similarly, for $K_0 = 3.5$ fm^{-1} ($E_d \simeq 37$ MeV) the nuclear region with density greater than $0.25\rho_N$ is important and for $K_0 = 3.0$ fm^{-1} ($E_d = 3$ MeV) the density threshold is down to $0.13\rho_N$.

These qualitative arguments were quite helpful in selecting the range of incident energies for which the Pauli breakup calculations were eventually done (Sec. VIII).

IV. FORMAL DERIVATION OF SOUND AND APPROPRIATE INTEGRAL EQUATIONS FOR DEUTERON INDUCED REACTIONS

Since the deuteron breakup is a three-body problem with the usual divergence difficulties, we seek a formulation for the reaction amplitude in the form of an integral equation with compact kernel. We refer to such a formulation as "sound." In addition we seek an "appropriate" formulation, i.e., one in which the contributions by the Pauli mechanism are essentially separated from the contribution by other mechanisms.

To enable ourselves to focus on the effects of the exclusion principle, and to allow the possibility of as transparent an analysis as is possible, we make some simplifying assumptions, discussed in an earlier report.[20]

With these assumptions, the asymptotic Hamiltonians for the incident channel can be written as $H_i = t_n + t_p + V_{np} = H_d$, while the complete Hamiltonian can be expressed as

$$\overline{H} = Q(H_d + V_n + V_p)Q = QH_dQ + \overline{V}_n + \overline{V}_p . \tag{4.1}$$

Here Q is a projection operator which projects onto the two-particle space spanned by products of unoccupied single-particle states of the target nucleus.

The integral equation obtained in Ref. 20 for the breakup amplitude when generalized to include other final channels, reads:

$$\tilde{U}^+_{fi} = W_f^{-\dagger}(v_f - w_f)W_i^+ + W_f^{-\dagger}(v_f - w_f)G_c(v_i - w_i)W_i^+ + \tilde{U}^+_{fi}G_i v_c G_c (v_i - w_i)W_i^+ . \tag{4.2}$$

Here w_i, w_f, and v_c are arbitrary potentials[21] to be chosen to obtain sound and appropriate integral equations for reaction amplitudes. The initial- (final-) state interactions $v_{i(f)}$ are defined by $v_{i(f)} = \overline{H} - H_{i(f)}$. The Green's functions G_c, G_i, and G_f are defined by

$$G_\alpha = [E_0^+ - (\overline{H} - V_\alpha)]^{-1} = [E_0^+ - H_\alpha]^{-1}, \quad \alpha = i, f, \text{ or } c . \tag{4.3}$$

The initial- and final-state distorted-wave operators are given by

$$W_i^+ = 1 + g_i w_i , \quad g_i = (E_0^+ - H_i - w_i)^{-1} , \tag{4.4}$$

and

$$W_f^{-\dagger} = 1 + w_f g_f , \quad g_f = (E_0^+ - H_f - w_f)^{-1} . \tag{4.5}$$

The tilde sign over U^+_{fi} is a reminder that Eq. (4.2) can be used for evaluation of reaction cross sections only if the final-state distortion potential w_f

is so chosen as to satisfy the condition

$$\langle f(E_0)|w_f g_f G_i^{-1}|i(E_0)\rangle = \lim_{\epsilon\to 0} i\epsilon\langle f|w_f g_f|i\rangle = 0 . \tag{4.6}$$

In Eq. (4.2), the obvious choice of a v_c that does not involve any of the two-body potentials in $(v_i - w_i)$ insures that there are no troublesome δ-function singularities in the kernel. As a result it has a chance of being a compact kernel.

V. DEUTERON BREAKUP

A. Selection of Arbitrary Potentials for the Breakup Problems

For our model breakup problem we have $v_i = \overline{H} - H_i = \overline{V}_n + \overline{V}_p + V_x$ and $v_f = \overline{H} - H_f = \overline{V}_n + \overline{V}_p + V_{np} + V_x$. Here V_x is the "exclusion potential" defined by $V_x = QH_dQ - H_d$, i.e., it is just the difference between uninhibited deuteron Hamiltonian and the exclusion principle restricted deuteron Hamiltonian. It can also be expressed as

$$V_x = -(PH_d + H_dP) + PH_dP , \tag{5.1}$$

where the projection operator P is complementary to Q, i.e., $P = 1 - Q$. In terms of the one-particle states of the target nucleus, P can be written as follows:

$$P = S_{i,\alpha,\beta}(|i(n)\alpha(p)\rangle\langle\alpha(p)i(n)| + |i(p)\beta(n)\rangle\langle\beta(n)i(p)|) . \tag{5.2}$$

Here index i runs over all one-particle states, α runs over states occupied in the target nucleus by protons, and β runs over states occupied by neutrons. The symbol S denotes summation over discrete states and integration over continuum of states. The letters n, p in the parentheses refer to neutron and proton coordinates. In writing Eq. (5.2) we have used the assumption that the target nucleus can be adequately represented by a single Slater determinant of one-particle states.

Here we choose the final-state distortion potential to be $w_f = V_{np}$, so that from Eq. (4.5) the final-state distortion wave operator is

$$W_f^{-\dagger} = 1 + V_{np}g_f, \quad g_f = (E_0^+ - H_0 - V_{np})^{-1} = G_i . \tag{5.3}$$

Thus the condition (4.6) reduces to $\langle f(E_0)|V_{np}|(i(E_0)\rangle = 0$, which is obviously satisfied as the initial and final states have different magnitude for deuteron center-of-mass momentum, whereas V_{np} is diagonal in that coordinate.

With the choice (governed by our desire to exhibit the Pauli mechanism in an explicit manner in the final integral equation) $w_i = \overline{V}_n + \overline{V}_p$, the most appropriate intermediate coupling potential, v_c, which will make the kernel of the integral Eq. (4.2) compact, is found to be $v_c = QV_{np}Q = \overline{V}_{np}$. The Green's function G_c associated with this choice of v_c is

$$G_c = (E_0^+ - H_c)^{-1} = [E_0^+ - Q(H_0 + V_n + V_p)Q]^{-1} . \tag{5.4}$$

With these choices, our integral Eq. (4.2) for breakup amplitude becomes

$$U_{od}^+ = W_f^{-\dagger}(\overline{V}_n + \overline{V}_p)W_i^+ + W_f^{-\dagger}(V_x + V_xG_cV_x)W_i^+ + W_f^{-\dagger}(\overline{V}_n + \overline{V}_p)G_cV_xW_i^+ + \tilde{U}_{od}^+ G_i\overline{V}_{np}G_cV_xW_i^+ . \tag{5.5}$$

Here, the wave operator W_i^+ is found from its defining Eq. (4.4) to be (after substituting $W_i = \overline{V}_n + \overline{V}_p$)

$$W_i^+ = 1 + (E_0^+ - H_i - \overline{V}_n - \overline{V}_p)^{-1}(\overline{V}_n + \overline{V}_p) = W_{n+p}^+ . \tag{5.6}$$

The kernel of Eq. (5.5) is compact (Appendix B). As a result, the inhomogeneous terms may be expected to provide a mathematically meaningful first approximation to the full transition amplitude $\tilde{U}_{fi}^+$. We now proceed to discuss these inhomogeneous terms.

B. Pauli Breakup Amplitude

In Eq. (5.5), the second set of inhomogeneous terms,

$$(U_{od}^0)_p = W_f^{-\dagger}(V_x + V_xG_cV_x)W_i^+ , \tag{5.7}$$

are specific to the effects of Pauli exclusion, in the sense that of all potentials in the problem, they involve only the exclusion potential V_x directly. Also, in the limit of deuteron nucleus potential $(V_n + V_p)$ approaching zero, these are the only inhomogeneous terms that survive. We may therefore refer to Eq. (5.7) as the distorted-wave approximate Pauli breakup amplitude.

On the other hand, the first set of inhomogeneous terms of Eq. (5.5) give the exact breakup amplitude in a model without exclusion, i.e., when $Q \equiv 1$. The remaining set of inhomogeneous terms describe the leading cross terms between Pauli (V_x) and nuclear potential $(V_n + V_p)$ breakup.

Physically, the Pauli breakup [Eq. (5.7)] may be understood to describe the following sequence of events:

(1) The incoming deuteron wave is distorted by the wave operator W_i^+, which describes scattering of nucleons in the deuteron by the potentials $\overline{V}_n$ and $\overline{V}_p$.

(2) The deuterons are broken up by the exclusion potential V_x or successive applications of it with propagation under Green's function $G_c=[E_0^+-Q(H_0+V_n+V_p)Q]^{-1}$ in between.
(3) The outgoing neutron and proton scatter off each other through interaction V_{np}. This scattering is described by $W_f^{-\dagger}$.

We now proceed to derive similar equations for Pauli elastic scattering and stripping amplitudes.

VI. PAULI MECHANISM IN DEUTERON ELASTIC SCATTERING AND STRIPPING REACTIONS

A. Deuteron Elastic Scattering

In this case we cannot use Eq. (4.2), as condition (4.6) cannot be satisfied for any nontrivial potential w_f. Therefore, we work with a more general equation,[20]

$$U_{fi}^+=W_f^{-\dagger}(v_f-w_f)W_i^++W_f^{-\dagger}(v_f-w_f)G_c(v_i-w_i)W_i^++w_fg_fG_i^{-1}[1-G_iv_cG_c(v_i-w_i)W_i^+]+U_{fi}^+G_iv_cG_c(v_i-w_i)W_i^+, \tag{6.1}$$

in which both the initial- and final-state distortion potentials (w_i and w_f) are completely arbitrary. In order to exhibit the Pauli effects explicitly, we set

$$w_i=w_f=\overline{V}_n+\overline{V}_p$$

and

$$V_c=\overline{V}_{np},$$

to obtain

$$U_{dd}^+=(\overline{V}_n+\overline{V}_p)W_i^++W_i^{-\dagger}(V_x+V_xG_cV_x)W_i^+-(W_i^{-\dagger}-1)\overline{V}_{np}G_cV_xW_i^++U_{dd}^+G_i\overline{V}_{np}G_cV_xW_i^+. \tag{6.2}$$

In writing Eq. (6.2) we have used $w_fg_fG_i^{-1}=w_fW_i^+$ which can be easily verified. All operators other than $W_i^{-\dagger}$ have already been defined in Sec. V A. The wave operator $W_i^{-\dagger}$ is adjoint of W_i^{*+} and describes scattering of deuterons in the final channel by $(\overline{V}_n+\overline{V}_p)$.

In a manner analogous to the identification of Pauli breakup amplitude, from Eq. (6.2) we have distorted-wave approximate (DWA) Pauli elastic scattering amplitude given by

$$(U_{dd}^0)_p=W_i^{-\dagger}(V_x+V_xG_cV_x)W_i^+. \tag{6.3}$$

The major source of difficulty in evaluating the Pauli elastic scattering amplitude are the distortion-wave operators W_i^+ and $W_i^{-\dagger}$, both of which describe scattering of deuteron plane waves by potentials $(\overline{V}_n+\overline{V}_p)$. The attenuated accelerated plane-wave-approximation method of Sec. VII could be used for both the initial- and final-state distortion-wave operators. However, the error involved in using the above-mentioned approximation is liable to be much more serious here than in the case of breakup where it has to be used only in the initial-state distortion. For this reason, we shall report calculated results only for Pauli breakup.

B. Deuteron Stripping Reaction

Turning to the problem of deuteron stripping, we shall consider only the neutron stripping, i.e., the reaction $A+d\rightarrow(A+n)+p$. The corresponding equations for proton stripping can be obtained in an analogous manner. In this case we have the asymptotic Hamiltonian for the final channel given by

$$H_f=Q(t_n+V_n)Q+t_p, \tag{6.4}$$

so that the final-state interaction is $v_f=H-H_f=\overline{V}_p+V_{np}+V_x'$, where

$$V_x'=Q(t_p+V_{np})Q-(t_p+V_{np}). \tag{6.5}$$

Here we use Eq. (4.2) for $\tilde{U}_{fi}^+$ with the choice $w_i=\overline{V}_n+\overline{V}_p$, $w_f=\overline{V}_p$, and $V_c=\overline{V}_{np}$. Then

$$\tilde{U}_{pd}^+=W_p^{-\dagger}V_{np}W_i^++W_p^{-\dagger}(V_x'+V_x'G_cV_x)W_i^++W_p^{-\dagger}V_{np}G_cV_xW_i^++U_{pd}^+G_i\overline{V}_{np}G_cV_xW_i^+. \tag{6.6}$$

The only undefined object in Eq. (6.6) is the final-state distortion-wave operator $W_p^{-\dagger}$. From defining Eq. (4.5) with $w_f=\overline{V}_p$ we have

$$W_p^{-\dagger}=1+\overline{V}_p(E_0^+-H_f-\overline{V}_p)^{-1}. \tag{6.7}$$

Since we have used truncated transition operator $\bar{U}^{+}_{fi}$, our choice of w_f must satisfy condition (4.6). Potential $\bar{V}_p$ involves only the coordinates of proton with respect to the target and therefore, cannot cause transitions back to the initial channel in which neutron and proton are bound together. The matrix element in the second member of Eq. (4.6) is therefore finite and the choice $w_f = \bar{V}_p$ is consistent with condition (4.6).

As before, we identify the DWA Pauli stripping amplitude to be

$$(U^0_{pd})_p = W^{-\dagger}_p (V'_x + V'_x G_c V_x) W^{+}_i . \tag{6.8}$$

The calculation of this amplitude is again an involved one and has been postponed until suitable methods for evaluating or approximating the initial- and final-state distorted-wave operators have been developed.

We now proceed to derive an approximate formula for the Pauli breakup cross section for the purpose of numerical results.

VII. APPROXIMATE CALCULATION OF PAULI BREAKUP CROSS SECTION

A. General Discussion of Approximations Used

On the basis of Eq. (5.7) we proceed to estimate the Pauli breakup cross section. The purpose is to obtain some semiquantitative insight into the specific features of the Pauli mechanism. This limited purpose is consistent with the several approximations we shall make in order to obtain numerical results. One expects these simplifications to involve errors, but hopefully, not such as to distort beyond recognition the major over-all magnitudes and specific qualitative features of angle and energy dependence.

The approximations make in calculating the Pauli breakup amplitude are as follows:

(1) The (small) second-order term in Eq. (5. 7) is neglected. This is because V_x has finite matrix elements only in the space complimentary to Q, and $H_c = Q(H_0 + V_n + V_p)Q$ (in the Green's function, G_c) has matrix elements only in the space Q. Thus, the only nonvanishing contributions to this term occur with the energy denominator equal to the total energy, and should therefore be small compared with the term retained.

(2) The initial-state distorted wave $W^{+}_i|\,\phi_0 \vec{K}_0\rangle$ is approximated by an attenuated deuteron plane wave $N|\,\phi_0 \vec{K}^{+}_0\rangle$. One is led to this approximation by the fact that one needs a good representation of the initial-state distorted wave only in the interior of the nucleus and the following considerations:

(a) Assume that $(\bar{V}_n + \bar{V}_p)$ can be replaced by a deuteron optical potential $V(r_d) + iW(r_d)$.

(b) Assume that the imaginary part of the optical potential reduces the amplitude of the deuteron wave in the interior by a factor, N, less than 1.

(c) Neglect the focusing effects[22] of the spherical nucleus on the incoming wave and replace the wave function inside by a plane wave with a wave number K^{+}_0 corresponding to kinetic energy $E_0 + \epsilon_0 + \bar{V}_0$. Here $\bar{V}_0$ is the average well depth of the real part of deuteron target optical potential. With these approximations, from Eq. (5.7) we get

$$\langle \vec{k}' \vec{K}'|(U^0_{0d})_p|\phi_0 \vec{K}_0\rangle = N\langle \chi^{-}_{\vec{k}'} \vec{K}'|V_x|\,\phi_0 \vec{K}^{+}_0\rangle , \tag{7.1}$$

where $\vec{k}', \vec{K}'$ are relative and center-of-mass momenta of the final out-going particles; $\vec{K}_0$ is the momentum of incident deuteron and ϕ_0 is the internal wave function of the deuteron. The scattering state $\langle \chi^{-}_{\vec{k}'} \vec{K}'|$ $= \langle \vec{k}' \vec{K}'|W^{-\dagger}_f$ is an eigenstate of the Hamiltonian H_d with the same energy as that of the state $\langle \vec{k}' \vec{K}'|$, by virtue of Eq. (5.3) for the wave operator. Now on substituting Eq. (5.1) for V_x one gets

$$\frac{1}{N}\langle \vec{k}' \vec{K}'|(U^0_{0d})_p|\,\phi_0 \vec{K}_0\rangle \simeq -(2E_0 + \bar{V}_0)\langle \chi^{-}_{\vec{k}'} \vec{K}'|\,P|\,\phi \vec{K}^{+}_0\rangle + \langle \chi^{-}_{\vec{k}'} \vec{K}'|\,PH_d\,P|\,\phi \vec{K}^{+}_0\rangle . \tag{7.2}$$

Here E_0 is the total energy of the incident deuteron as well as that of the outgoing particles. The actual calculations were performed with

$$\frac{1}{N}\langle \vec{k}' \vec{K}'|(U^0_{0d})_p|\,\phi_0 \vec{K}_0\rangle = -2(E_0 + \bar{V}_0)\langle \vec{k}' \vec{K}'|\,P|\,\phi_0 \vec{K}^{+}_0\rangle + \langle \vec{k}' \vec{K}'|\,PH_d\,P|\,\phi_0 \vec{K}^{+}_0\rangle \tag{7.3}$$

which is obtained from Eq. (7.2) when the third approximation, below, is invoked.

(3) The final-state distortion due to $w_f = V_{np}$ is neglected (see Appendix C) and $\langle \chi^{-}_{\vec{k}'}|$ is replaced by $\langle \vec{k}'|$.

B. Approximate Pauli Amplitude for $N = Z$ Target

In this case the projection operator P becomes [from Eq. (5.2)]

$$P=\sum_{i,\alpha}[|i(n)\alpha(p)\rangle\langle\alpha(p)i(n)|+|i(p)\alpha(n)\rangle\langle\alpha(n)i(p)|]. \tag{7.4}$$

Here i runs over all one-particle states and α runs over only the occupied one-particle states of the target nucleus.

Notice that, for the present case of $N=Z$, in Eq. (7.3) for the Pauli breakup amplitude, three objects are invariant under the exchange of neutron and proton space coordinates. These are the initial state, which is space symmetric, the projection operator P, and the Hamiltonian H_d. Therefore, only the space-symmetric part of the final state will contribute to Eq. (7.3) for the Pauli breakup amplitude. As a result the amplitude will be invariant under the transformation $\vec{k}'\to-\vec{k}'$.

With the operator P given by Eq. (7.4), we have for the first matrix element on the right-hand side of Eq. (7.3),

$$\langle\vec{k}'\vec{K}'|P|\phi_0\vec{K}_0^+\rangle=\phi_0(\vec{k}'+\tfrac{1}{2}\vec{Q})\sum_\alpha\psi_\alpha^*(\vec{k}_-'-\vec{Q})\psi_\alpha(\vec{k}_-')+\phi_0(\vec{k}'-\tfrac{1}{2}\vec{Q})\sum_\alpha\psi_\alpha^*(\vec{k}_+'-\vec{Q})\psi_\alpha(\vec{k}_+'), \tag{7.5}$$

where $\vec{Q}=\vec{K}'-\vec{K}_0^+$ is the effective center-of-mass momentum transfer and $\vec{k}_\pm'=\frac{1}{2}\vec{K}\pm\vec{k}'$ are the momenta of the outgoing particles.

We evaluate the second matrix element in Eq. (7.3) (i.e., the matrix element of PH_dP) in two parts. First we evaluate the matrix element of PH_0P and then that of $PV_{np}P$:

$$\begin{aligned}\langle\vec{k}'\vec{K}'|PH_0P|\phi_0\vec{K}_0^+\rangle=\int d^3\vec{k}\left(\frac{k_-'^2+k^2}{2}\right)\sum_\alpha\psi_\alpha^*(\vec{k}_+')\psi_\alpha(\vec{k})\\ \times[\phi_0(\tfrac{1}{2}\vec{K}_0^+-\vec{k}_-')\sum_\alpha\psi_\alpha^*(\vec{K}_0^+-\vec{k}_-')\psi_\alpha(\vec{k})+\phi_0(\vec{k}-\tfrac{1}{2}\vec{K}_0^+)\sum_\alpha\psi_\alpha^*(\vec{K}_0^+-\vec{k})\psi_\alpha(\vec{k}_-')]\\ +(\text{same term but with }\vec{k}'\text{ replaced by }-\vec{k}').\end{aligned} \tag{7.6}$$

For V_{np} we shall use the separable potential defined in Sec. III, and obtain for its matrix element

$$\begin{aligned}\langle\vec{k}'\vec{K}'|PV_{np}P|\phi_0\vec{K}_0^+\rangle=-\int d^3\vec{k}d^3\vec{K}f(\tfrac{1}{2}\vec{K}-\vec{k}_-')\sum_\alpha\psi_\alpha(\vec{K}-\vec{k}_-')(\vec{k}_+')\\ \times f(\vec{k})\langle\vec{k}\vec{K}|P|\phi_0\vec{K}_0^+\rangle+(\text{same term but with }\vec{k}'\text{ replaced by }-\vec{k}').\end{aligned} \tag{7.7}$$

When Eq. (7.5) is used to expand the last factor in Eq. (7.7), both Eqs. (7.6) and (7.7) are seen to involve two nuclear state summands and some extra integrations. Further progress can be made only by introducing a specific model for the occupied nuclear states. We therefore turn to the specific case of ^{16}O.

The specific case of ^{16}O. For this case we use the isotropic harmonic-oscillator wave functions for the occupied nuclear states. These wave functions in Cartesian representation are

$$\psi_{n_x,n_y,n_z}(\vec{r})=C_{n_x}C_{n_y}C_{n_z}H_{n_x}(\alpha_0x)H_{n_y}(\alpha_0y)H_{n_z}(\alpha_0z)e^{-r^2\alpha_0{}^2/2}, \tag{7.8}$$

where α_0 is the inverse range parameter and n_x, n_y, n_z are quantum numbers for this state. H_n denotes Hermite polynomial of order n. The normalization constants, C's, are given by $C_n=(\alpha_0/\pi^{1/2}2^nn!)^{1/2}$. The Fourier-transformed wave function can be written as

$$\psi_{n_x,n_y,n_z}(\vec{k})=\frac{i^N}{\alpha_0^3}C_{n_x}C_{n_y}C_{n_z}H_{n_x}(k_x/\alpha_0)H_{n_y}(k_y/\alpha_0)H_{n_z}(k_z/\alpha_0)e^{-k^2/2\alpha_0{}^2}, \tag{7.9}$$

where N is the sum of quantum numbers n_x, n_y, n_z.

The actual nuclear wave functions are eigenstates of angular momentum, L^2. However, for the present purpose, we need not evaluate them, as we need summands of $\psi^*\psi$ over complete shells, and the result will be the same whether we use Cartesian wave functions or spherical wave functions (eigenfunctions of L^2).

For ^{16}O there are only four levels involved: (0, 0, 0), (1, 0, 0), (0, 1, 0), and (0, 0, 1). The numbers in parentheses are, respectively, the n_x, n_y, and n_z values. Using Eq. (7.9), we obtain

$$\sum_\alpha\psi_\alpha^*(\vec{k}_1)\psi_\alpha(\vec{k}_2)=\frac{C_0^6}{\alpha_0^6}\left(1+\frac{C_1^2}{C_0^2\alpha_0^2}\vec{k}_1\cdot\vec{k}_2\right)e^{(-\vec{k}_1{}^2+\vec{k}_2{}^2)/2\alpha_0{}^2}. \tag{7.10}$$

Once substitution from Eq. (7.10) is made, the integral involved in the matrix element of PH_0P [Eq. (7.6)] can be carried out exactly. However, the integrals in the matrix element of $PV_{np}P$ [Eq. (7.7)] could not be carried out exactly. An approximate method was used to evaluate these integrals (see Appendix D).

The final result is

$$\frac{1}{N}\langle \vec{k}'\vec{K}'|(U_{0d}^0)_p|\,\phi_0\vec{K}_0\rangle \simeq T_1+T_2+T_3+\langle \vec{k}'\vec{K}'|\,PV_{np}P|\,\phi_0\vec{K}_0^+\rangle . \tag{7.11}$$

Here the first term is

$$T_1=\frac{\phi_0(\vec{k}'-\frac{1}{2}\vec{Q})}{\alpha_0{}^3\pi^{3/2}}\exp(-A_1/\alpha_0{}^2)\{\tfrac{1}{2}\alpha_0{}^2+[2E_0+\overline{V}_0-\tfrac{1}{2}k_-'^2-\tfrac{5}{4}\alpha_0{}^2][1+2(A_1-\tfrac{1}{2}Q^2)/\alpha_0{}^2]\}\,, \tag{7.12}$$

while T_2 can be obtained from T_1 by the transformation $\vec{k}'\to-\vec{k}'$,

$$T_2=\frac{-\phi_0(\vec{k}'+\frac{1}{2}\vec{Q})}{\alpha_0{}^3\pi^{3/2}}e^{-A_2/\alpha_0{}^2}\{\tfrac{1}{2}\alpha_0{}^2+(2E_0+\overline{V}_0-\tfrac{1}{2}k_+'^2-\tfrac{5}{4}\alpha_0{}^2)[1+2(A_2-\tfrac{1}{2}Q^2)/\alpha_0{}^2]\} \tag{7.13}$$

and T_3 is given by

$$T_3=\frac{4\pi}{\alpha_0{}^6\pi^3}e^{-A_3/\alpha_0{}^2}[I_2A_0A_3+I_4(A_0-4A_3\vec{k}_+'\cdot\vec{k}_-'/3\alpha_0{}^4)+4I_6\vec{k}_+'\cdot\vec{k}_-'/3\alpha_0{}^4]\,. \tag{7.14}$$

The new quantities introduced in the preceding three equations are

$$A_1=(\tfrac{1}{2}\vec{K}_0^+ +\vec{k}')^2+\tfrac{1}{4}Q^2\,, \tag{7.15}$$

$$A_2=(\tfrac{1}{2}\vec{K}_0^+ -\vec{k}')^2+\tfrac{1}{4}Q^2\,, \tag{7.16}$$

$$A_3=\tfrac{1}{4}K_0^{+2}+E_0\,, \tag{7.17}$$

$$A_0=(1+\vec{k}_+'\cdot\vec{K}_0^+/\alpha_0{}^2)(1+\vec{k}_-'\cdot\vec{K}_0^+/\alpha_0{}^2)\,, \tag{7.18}$$

and

$$I_n=\int_0^\infty k^n dk\,\phi_0(k)e^{-k^2/\alpha_0{}^2}\,. \tag{7.19}$$

In the last equation the integral is exactly evaluable in terms of the error functions of a/α_0 and k_0/α_0 when one substitutes for ϕ_0 from Eq. (3.3).

Evaluation of the $PV_{np}P$ term of Eq. (7.11) is discussed in Appendix D.

C. Relation Between Breakup Amplitude and Cross Section

Goldberger and Watson[23] give a general formula relating transition amplitude to the reaction cross sections. Applied to the deuteron breakup problem it reads

$$\Delta\sigma=\int d^3\vec{k}_n\,d^3\vec{k}_p\,d^3\vec{K}_T\,\delta^3(\vec{P}_f-\vec{P}_i)\delta(E_f-E_i)(2\pi)^4\frac{|T_{fi}|^2}{v_0}\,. \tag{7.20}$$

Integration is over a small volume in the nine-dimensional momentum space about the point $(\vec{k}_n,\vec{k}_p,\vec{K}_T)$. Here k_n, k_p, and K_T are the momenta of the proton, neutron, and the target, respectively, in the final state. P_i and P_f are the total momenta of the initial and final systems, respectively. E_f is the energy of the final system and E_i that of the initial system. T_{fi} is the transition amplitude and $v_0=\frac{1}{2}K_0$ is the velocity of incident deuteron with respect to the target.

We write $d^3k_p=k_p\,d\epsilon_p\,d\Omega_p$ and likewise for d^3k_n. Then we note that the d^3K_T integration takes care of momentum δ function. The $d\epsilon_n$ integration can be used to eliminate the energy δ function with the result that

$$\Delta\sigma=\int k_p\,d\epsilon_p\,d\Omega_p\,k_n\,d\Omega_n\frac{2}{K_0}(2\pi)^4|T_{fi}|^2\,. \tag{7.21}$$

Here k_n is determined by energy conservation equation, i.e.,

$$\tfrac{1}{2}k_n{}^2=\tfrac{1}{4}K_0{}^2-\epsilon_0-\tfrac{1}{2}k_p{}^2 \tag{7.22}$$

and it is understood that the transition operator is evaluated between energy conserving states.

Finally, we can write for the triple-differential cross section

$$\frac{d^3\sigma}{d\Omega_n d\Omega_p d\epsilon_p} = \frac{32 k_n k_p \pi^4}{K_0} |T_{fi}|^2 \tag{7.23}$$

in units where $\hbar = M = 1$. When the momenta are measured in units of fm^{-1}, one need divide the results by 4.15 to obtain cross section in mb/sr^2 MeV. The phase-space factor [the factor multiplying $T_{fi}{}^2$ in Eq. (7.23)] under the energy conservation condition [Eq. (7.22)] is maximum for $k_n = k_p$ and decreases monotonically to zero on either side.

We now proceed to the discussion of numerical calculations and results.

VIII. NUMERICAL ESTIMATES OF PAULI BREAKUP

A. Input Parameters

The isotropic oscillator parameter [see Eq. (7.8)] for ^{16}O wave functions is taken[24] to be given by $\alpha_0{}^{-1} = 1.76$ fm. For the deuteron we take a Yamaguchi-type one-term separable potential [Sec. III, Eq. (3.1)] with $a = 0.9$ fm^{-1} and $g^2 = 0.11677$ fm^{-3} chosen to fit the binding energy and mean square radius of the deuteron (Appendix A).

For the deuteron nucleus optical potential,[25] we assume a volume absorption and take $V_0 = 80$ MeV and $W_0 = 15$ MeV, both assumed to be constant over the nuclear volume described by a sphere of radius $R = 3.6$ fm. With this input, K_0^+ can be trivially determined for a given incident energy.

The average cross-section reduction factor due to absorption for an undeflected trajectory with impact parameter b is $N^2(b) = (1/2z_0)\int^{z_0} N^2(b,z)dz$, where $z_0{}^2 = R^2 - b^2$ and

$$N^2(b,z) = \exp\left(-\int_{-z_0}^{z} \frac{4MW_0}{\hbar^2 K_0^+}\, dx\right) = \exp\left(-\frac{4MW_0(z+z_0)}{\hbar^2 K_0^+}\right). \tag{8.1}$$

The over-all average cross-section reduction factor, $N^2 = (1/\pi R^2)\int_0^R N^2(b) 2\pi b\, db$, is then found to be given by[26]

$$N^2 = (2/\lambda^2)\left[\lambda - 1 + e^{(-\lambda)}\right], \quad \lambda = 8MW_0 R/\hbar^2 K_0^+ . \tag{8.2}$$

For 90-MeV incident energy (for which V_0, W_0 are given above) Eq. (8.2) gives $N^2 = 0.5002$. Since W_0 and K_0^+ both increase with incident energy, the values of N^2 at other incident energies for which calculated results are reported are about the same.

B. Some Properties of Pauli Breakup on ^{16}O

Before we go on to discuss the numerical results, it is worthwhile to point out some important features one can expect on the basis of Eqs. (7.11)–(7.19) and (7.23), which comprise the formula for Pauli breakup cross section. In the expression for transition amplitude [Eqs. (7.11)–(7.19)], of all the functions involved, the exponentials are the most dominating ones. Therefore, to recognize the important properties of the transition amplitude, we look at the exponential factors first.

The arguments of the exponentials involved in the transition amplitude terms T_1, T_2, and T_3 are, respectively, $-A_1/\alpha_0{}^2$, $-A_2/\alpha_0{}^2$, and $-A_3/\alpha_0{}^2$. For large amplitude, A_1 and A_2 both require that $\vec{Q}$, the effective momentum transfer, be small. A_1 is further reduced if $\vec{k}' \simeq \frac{1}{2}\vec{K}_0^+$, while A_2 requires that these vectors be equal and opposite. A_3 is independent of the directions of the initial and final momenta and is always large.

The structure of the exponentials in the fourth term, the $PV_{np}P$ term, is similar to that of the exponentials in T_1 and T_2 (see Appendix D). However, this term, T_4, is found to be much smaller than $T_1 + T_2$. Physically, the damping of T_4 in comparison to $T_1 + T_2$ can be understood as follows. The part of phase space that contributes to the matrix elements of $T_1 + T_2$ is restricted only in the coordinates of one particle at a time, while their relative coordinate is restricted only by the finite size of the deuteron wave function. In case of the matrix elements of $PV_{np}P$, the contributing phase space is further restricted in the relative coordinate due to the short-range nature of V_{np}.

Thus we conclude that T_1 and T_2 are the only terms that can have large magnitudes. Therefore in the regions of large cross sections, the variation of Pauli breakup with momenta of outgoing particles is governed mainly by them. We therefore conclude that:

(a) The Pauli breakup cross section is large only for values of the effective momentum transfer ($\vec{Q} = \vec{K}_0^+ - \vec{k}'$) which are at most a few times α_0.

(b) It is further required that $\vec{k}'$ be of the order of $\frac{1}{2}\vec{K}_0^+$ in magnitude and be as nearly along $\vec{K}_0$ (paral-

lel or antiparallel) as possible. The large magnitude of $\vec{k}'$ implies that the momenta of the outgoing particles $(\frac{1}{2}\vec{K}' \pm \vec{k}')$ will be very unequal. Also, large values of k', by energy conservation, imply small values of K'. This in turn, in general, implies large value of $\vec{Q} = \vec{K}_0^+ - \vec{K}'$. Thus (a) and (b), to some extent, compete against each other.
(c) Note that when $\vec{Q}$ is small and $|\vec{k}'| \simeq \frac{1}{2}K_0^+$ [when conditions (a) and (b) are nearly satisfied], the deuteron wave function in T_1 and T_2 has to be evaluated at approximately $\frac{1}{2}K_0^+$. Thus considerations (a) and (b) have to compete against the availability of large relative momenta in the deuteron wave function ϕ_0. However, since ϕ_0 is not as dominant a function as the Gaussian exponentials which bring about (a) and (b), this consideration (c) is of much lesser consequence.
(d) In evaluating the cross sections, the square of the transition amplitude has to be multiplied by the phase-space factor which is maximum for $k_n = k_p$ and monotonically decreases to zero on either side. Thus the phase-space factor also works against the effect (b) above and is particularly important near the end points of the spectrum, i.e., where either k_n or k_p is approaching zero.
(e) In regions of small cross sections, e.g. for the case of symmetric partition of energy, $\epsilon_p/E_0 \simeq \frac{1}{2}$, interference effects between various terms can cause the violation of (a), (b) which are based on T_1 or T_2 being large.

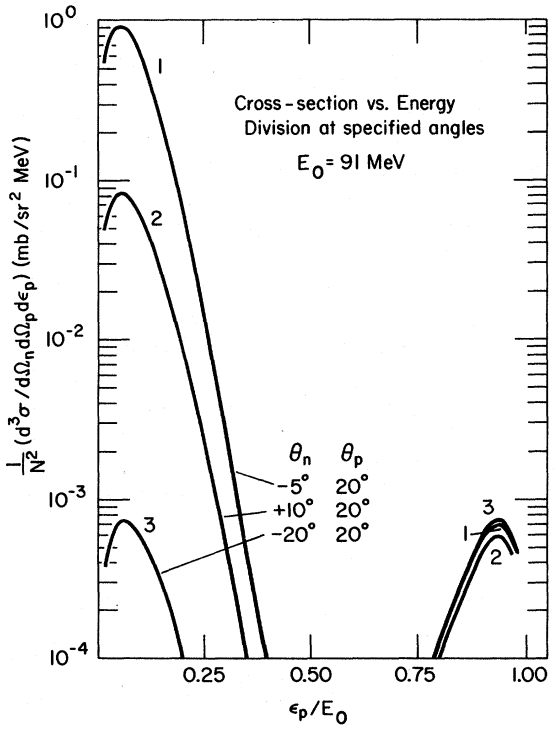

FIG. 4. The triple-differential cross section vs the fraction (ϵ_p/E_0) of energy carried by the proton for specific values of angles (θ_p, θ_n) are plotted for the case of incident energy $E_0 = 91$ MeV. By energy conservation $\epsilon_n/E_0 = 1 - \epsilon_p/E_0$. The specific cross-section reduction factors, $N^2 \sim 0.5$, due to absorption are suppressed in these plots, as indicated by the vertical axis label.

C. Energy Correlations Among the Breakup Products

These are depicted in Fig. 4 which shows the variation of $d^3\sigma/d\Omega_n\, d\Omega_p\, d\epsilon_p$ with $x = \epsilon_p/E_0$, the fraction of energy carried by the outgoing proton. These curves are drawn for fixed values of θ_n, θ_p, the angles at which the neutron and proton are observed.

From these curves we observe that the cross sections are maximal for very asymmetric partition of energy among the outgoing particles. The maxima in these curves are a clear demonstration of the property (b) of the Pauli breakup in competition with properties (a), (c), and (d) (these properties are discussed in the preceding section).

Each curve has two maxima. One of these corresponds to the situation where term T_1 [Eq. (7.12)] of the breakup amplitude is maximal, while the other corresponds to the situation where T_2 [Eq. (7.13)] is maximal. Since they attain maximal values for equal but opposite values of $\vec{k}'$, the two maxima are equally spaced from $x = \frac{1}{2}$. That is they correspond to conjugate values of x, e.g. x_1 and $1 - x_1$.

In the curves with $\theta_p = |\theta_n|$, $(20°, -20°)$, the heights of both maxima are equal in agreement with the invariance of the Pauli breakup amplitude under the transformation $\vec{k}' \to -\vec{k}'$. For the present case, this implies identical cross sections for $\epsilon_p/E_0 = x, 1 - x$. In the curves with $\theta_p \neq |\theta_n|$, $(20°, -5°; 20°, 10°)$, the maxima at lower value of $x = x_l$ is orders of magnitude higher than the maxima at the higher (conjugate) value $x_h = 1 - x_l$. It can be easily verified that $x_l < \frac{1}{2}$ corresponds to a lower value of effective momentum transfer $\vec{Q}$, than does the conjugate value $x_h = 1 - x_l$. These conjugate cases correspond to the same value of $|\vec{k}'|$ and to the same magnitudes of the final momenta but with the role of neutron and proton interchanged. The two cases differ, essentially, on account of $\vec{Q}$. The above mentioned result, therefore, is a manifestation of the strong (Gaussian) dependence of transition amplitudes on $\vec{Q}$.

D. Angular Correlations

The angular correlation curves (Fig. 5) show the variation of cross section with one of the scatter-

ing angles (here θ_p) when the other angle (here θ_n) and the energy carried by each of the out-going particles is considered to be fixed.

The interpretation of these curves in terms of the observations (a)–(e) of Sec. VIII B is complicated by the fact that all of these effects enter the picture simultaneously and in varying degrees depending on θ_n, θ_p, and x. However, combining the results of this figure with those of Fig. 4, one can conclude that the energy-integrated cross section $d^2\sigma/d\Omega_n\, d\Omega_p$ (for θ_n fixed at 10°) will consist of a superposition of a narrow peak centered at $\theta_p = 0°$ and a broad peak centered at $\theta_p \simeq \theta_n$, i.e., at θ_p corresponding to minimum total momentum transfer. The narrow central peak is very much reminiscent of the Serber[27] theory of deuteron breakup, which successfully explained the contemporary results of Helmholst, McMillan, and Swell.[28] The breakup mechanism in Serber theory essentially assumes complete physical exclusion of neutron and proton of the deuteron from the nuclear volume, whereas the Pauli breakup is based on a less restrictive exclusion, the Pauli exclusion. Therefore some similarities in the angular distributions in the two cases should not be very surprising.

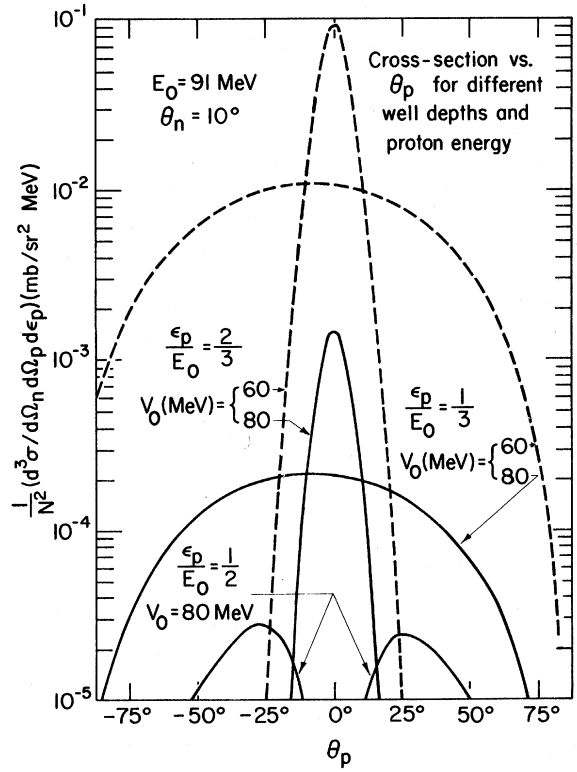

FIG. 5. The triple-differential cross section vs the proton angle θ_p in the forward 75° cone. The curves are labeled by the fraction of energy carried by the proton and the average depth of the real part of the deuteron nucleus optical potential. The strong dependence of results on the choice of V_0 is apparent. The reduction factor, $N^2 \sim 0.5$, is again suppressed as in Fig. 4.

E. Cross Section Versus T_d, the Deuteron Kinetic Energy in the Interior

From Sec. III and Fig. 2 it is clear that the cross section for Pauli breakup should strongly depend on T_d. Since $T_d = E_d + V_0$, where E_d is the incident deuteron's kinetic energy and V_0 is the well depth of the real part of deuteron-nucleus optical potential, we divide our discussion in two parts.

(a) Cross section versus V_0. The dotted curves in Fig. 5 correspond to the calculation with $V_0 = 60$ MeV instead of 80 MeV (solid curves). The increase in cross section by about 2 orders of magnitude shows the strong dependence of cross section on V_0 and hence on the momentum of the deuteron in the interior region. Thus our approximation, $W_i^+|\,\phi_0 K_0\rangle = N|\,\phi_0 K_0^+\rangle$ (which replaces the incident channel distorted wave by an attenuated but accelerated plane wave with a momentum which is the median of the momenta present in the distorted wave), gives an underestimate of the cross section. A more realistic estimate of the magnitude of the cross section would have been obtained if K_0^+ were replaced by some effective average $\bar{K}_0$ obtained by giving extra weight in the averaging process to the lower deuteron momenta in the distorted wave, $W_i^+|\,\phi_0 K_0\rangle$.

(b) Dependence of cross section on incident energy. We shall confine our attention only to the region of large cross sections (forward angles and small values of $x = \epsilon_p/E_0$), where $T_1 + T_2$ give the dominant contribution to the breakup amplitude (see Sec. VIII B). Since T_2 can be obtained from T_1 by the transformation $\vec{k}' \to -\vec{k}'$ and vice versa, they dominate the breakup amplitude in conjugate parts of the proton energy spectrum. Therefore, we need consider only one of them, say T_1, for the following discussion.

T_1 is dominated by e^{-A_1/α_0^2}. We rewrite A_1 in a form different from Eq. (7.15),

$$A_1 = [k_1^2 + (\vec{K}_0^+ - k_2)^2]/2\,, \tag{8.3}$$

where $\vec{k}_{1(2)} = \frac{1}{2}\vec{K}' \pm \vec{k}'$ are the momenta of the outgoing particles. Neglecting the deuteron binding energy we set $\frac{1}{2}k_1^2 \simeq E_d x_1$, $\frac{1}{2}k_2^2 \simeq E_d x_2$; $x_1 + x_2 = 1$. Also $\frac{1}{4}K_0^{+2} = E_d + V_0$, so that we can write

$$A_1 \simeq E_d + 2(E_d + V_0) - 2[2x_2 E_d(E_d + V_0)]^{1/2}\cos\theta_2\,. \tag{8.4}$$

Differentiating with respect to E_d, we obtain

$$\frac{dA_1}{dE_d} = 3 - 2\sqrt{x_2}\,\cos\theta_2\,\frac{2E_d + V_0}{[2E_d(E_d + V_0)]^{1/2}}\,. \tag{8.5}$$

Now T_1 is the dominant amplitude when [from Eq. (8.3)] k_1 is small ($x_1 \ll \frac{1}{2}$) and $\vec{k}_2$ is large and along the incident direction. In this region, therefore:
(i) Cross section will have exponential dependence on E_d.
(ii) The slope of semilog plot of cross section vs E_d will decrease linearly with $\sqrt{x_2}\cos\theta_2$. It slowly increases with E_d [Eq. (8.5)].
(iii) For the conjugate region ($x_2 \ll \frac{1}{2}$), the above results hold with the role of subscripts 1 and 2 interchanged.
These observations are clearly born out by Figs. 6 and 7.

F. Variation of Cross Sections with Nuclear Density

Figure 3 shows the variation of binding energy ($\bar{\epsilon}_0$) of a deuteron propagating through nuclear matter as a function of the nuclear matter density (ρ). The strong dependence of $\bar{\epsilon}_0$ on ρ suggests that the Pauli breakup cross sections will also vary drastically with the density nuclear matter inside the nucleus. For the oscillator model of ^{16}O, the local nuclear density is given by[24]

$$\rho(r) = \rho_0(1 + 2r^2\alpha_0^2)e^{-r^2\alpha_0^2} \text{ nucleons/unit volume}, \tag{8.6}$$

where ρ_0 is determined from normalization condition, $\int \rho\, d^3r = A = 16$, to be

$$\rho_0 = \alpha_0^3 A/4\pi^{3/2} \text{ nucleons/unit volume}. \tag{8.7}$$

Thus α_0, here, plays the role of Fermi momentum. Therefore, to study the dependence of Pauli breakup or nuclear density, triple differential cross section was calculated at several points with $\alpha^{-1} = 1.69$ fm and 1.83 fm instead of $\alpha_0^{-1} = 1.76$ fm. These new values of the parameter correspond to, roughly, ±12% change in ρ_0. The results are compared in Table I. The numbers in parentheses, below the cross sections with new parameters, are the factors by which the cross sections are enhanced or reduced by this 12% change in central density. The dominant effect of change in the value of α_0 comes from the exponential factors. The larger the numerators (A_1, A_2, A_3, etc.) of the negative exponents are, the larger the enhancement and reduction factors are expected to be. Hence these factors are larger where the cross sections are smaller and vice

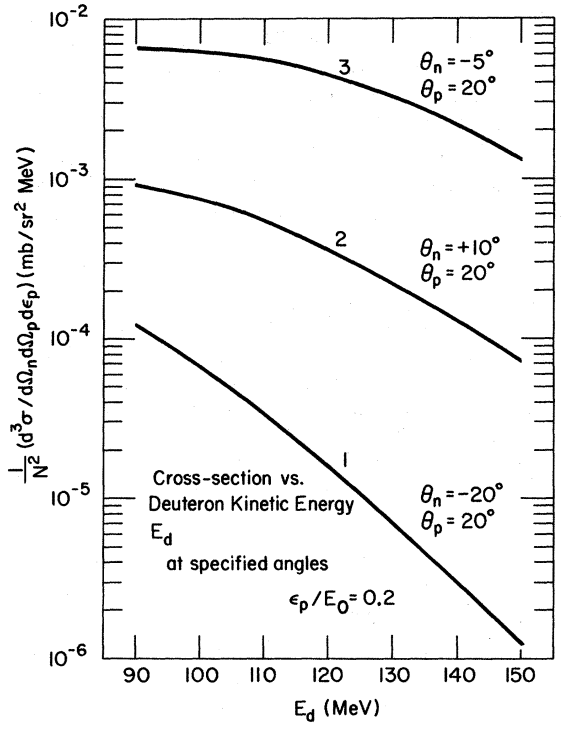

FIG. 6. The triple-differential cross section is plotted as a function of E_d (the kinetic energy of incident deuteron) at specified angles and fixed value of $\epsilon_p/E_0 = 0.2$. Note the decrease in the slope of the curves with increasing $\cos\theta_n$, i.e., in going from curves 1 to 2 to 3. Also notice the increase in the slope of each curve from left to right (cf., Sec. VIII E b).

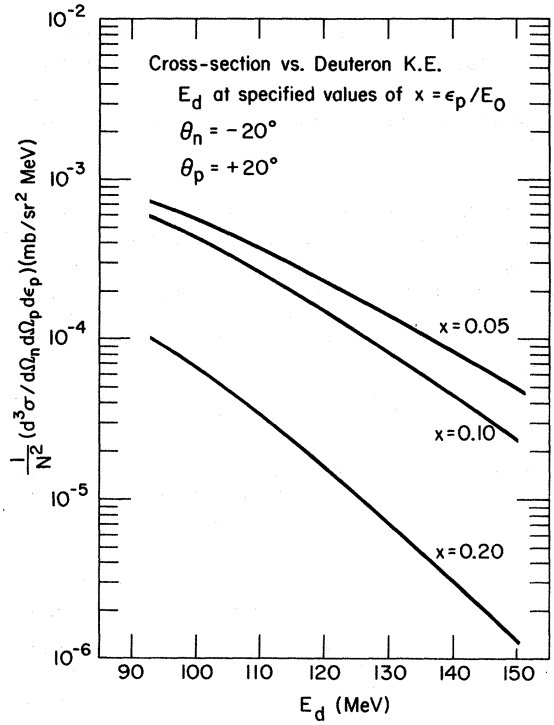

FIG. 7. The triple-differential cross section vs E_d at specified values of $x = \epsilon/E_0$, $\theta_n = -20°$, and $\theta_p = +20°$ being fixed. The gradual increase in slope of the curves with increasing values of x is apparent (cf. Sec. VIII E b).

TABLE I. Dependence of Pauli breakup on nuclear density. Values of cross section at selected points are compared for three values of oscillator model parameter for ^{16}O: $\alpha_0^{-1}=1.76$ fm, $\alpha_+^{-1}=1.69$ fm, and $\alpha_-^{-1}=1.83$ fm. The parameters $\alpha_\pm$ correspond to ±12% change in central nuclear density of ^{16}O. The numbers in parentheses below the cross sections for $\alpha^\pm$ are the enhancement or reduction factors corresponding to this ±12% change in ρ_0. These numbers speak for the strong dependence of Pauli breakup on ρ_0. (Cf. Sec. VIII F.)

Oscillator model parameter	ϵ_p/E_0	$d^3\sigma/d\Omega_n\, d\Omega_p\, d\epsilon_p$ mb/sr^2 MeV at the following points: $E_0=91$ MeV, $\theta_p=20°$, $\theta_n \to -20°$	$E_0=91$ MeV, $\theta_p=20°$, $-5°$	$E_0=91$ MeV, $\theta_p=20°$, $+10°$	$E_0=125$ MeV, $\theta_p=20°$, $\theta_n \to -20°$	$E_0=125$ MeV, $\theta_p=20°$, $-5°$	$E_0=125$ MeV, $\theta_p=20°$, $+10°$
α_+	0.05	0.1919×10^{-2}	0.1848×10^{1}	0.1747×10^{0}	0.4915×10^{-3}	0.1076×10^{1}	0.8761×10^{-1}
		(2.627)	(1.979)	(2.080)	(2.995)	(2.089)	(2.224)
α_0		0.7289×10^{-3}	0.9339×10^{0}	0.8400×10^{-1}	0.1641×10^{-3}	0.5150×10^{0}	0.3940×10^{-1}
α_-		0.2424×10^{-3}	0.4452×10^{0}	0.3797×10^{-1}	0.4708×10^{-4}	0.2321×10^{0}	0.1662×10^{-1}
		(3.007)	(2.098)	(2.212)	(3.486)	(2.219)	(2.371)
α_+	0.20	0.4104×10^{-3}	0.1747×10^{0}	0.2528×10^{-1}	0.4954×10^{-4}	0.1137×10^{0}	0.8529×10^{-2}
		(4.084)	(2.728)	(2.868)	(5.392)	(3.163)	(3.364)
α_0		0.1005×10^{-3}	0.6404×10^{-1}	0.8815×10^{-2}	0.9187×10^{-5}	0.3595×10^{-1}	0.2535×10^{-2}
α_-		0.1691×10^{-4}	0.2174×10^{-1}	0.2812×10^{-2}	0.1008×10^{-5}	0.1049×10^{-1}	0.6881×10^{-3}
		(5.943)	(2.946)	(3.135)	(9.114)	(3.427)	(3.684)

versa. The large values of these factors for small changes in ρ_0 bears out our earlier qualitative predictions regarding strong dependence of cross section on nuclear density.

G. Dependence of Results on Choice of Parameters for the Deuteron

In our model of the deuteron we found (Appendix A) that a whole range of combinations of the values for parameters a and g, which give rise to the same binding energy but give for the mean square radius $\langle r^2\rangle$, values between 18.7 and 14.2 fm.[2] These combinations satisfy the condition that the dimensionless quantity (g^2/a^3) be a constant.

On account of these ambiguities, it is both instructive as well as desirable to check on the dependence of the Pauli breakup cross sections on the choice of the above-mentioned parameters. With this in mind, in the region of large cross sections, some of the results were recalculated with $a=1.3$ fm^{-1} and $g^2=0.308\,98$ fm^{-3} replacing

TABLE II. Dependence of results on the choice of deuteron parameters. Calculated results at selected points are compared for two sets of deuteron parameters $-a=0.9$ fm^{-1}, $g=0.341\,72$ fm$^{-3/2}$ and $a'=1.3$ fm^{-1}, $g'=0.555\,86$ fm$^{-3/2}$. Both sets correspond to the same deuteron binding energy but slightly different values of mean square radius. The numbers in parentheses are percentage deviations of cross sections with a', g' from those corresponding to a, g. These numbers show that the cross sections do not depend critically on the parameters of the deuteron model (Cf. Sec. VIII G).

Parameters of deuteron model	ϵ_p/E_0	$d^3\sigma/d\Omega_n\, d\Omega_p\, d\epsilon_p$ mb/sr^2 MeV at the following points: $E_0=91$ MeV, $\theta_p=20°$, $\theta_n \to -20°$	$E_0=91$ MeV, $\theta_p=20°$, $-5°$	$E_0=91$ MeV, $\theta_p=20°$, $+10°$	$E_0=125$ MeV, $\theta_p=20°$, $\theta_n \to -20°$	$E_0=125$ MeV, $\theta_p=20°$, $-5°$	$E_0=125$ MeV, $\theta_p=20°$, $+10°$
a, g	0.05	0.7289×10^{-3}	0.9339×10^{0}	0.8400×10^{-1}	0.1641×10^{-3}	0.5150×10^{0}	0.3940×10^{-1}
a', g'		0.9519×10^{-3}	0.8092×10^{0}	0.8189×10^{-1}	0.2279×10^{-3}	0.4636×10^{0}	0.4066×10^{-1}
		(+30.6)	(−13.4)	(−2.5)	(+38.8)	(−10.0)	(+3.2)
a, g	0.10	0.5853×10^{-3}	0.6222×10^{0}	0.6068×10^{-1}	0.1000×10^{-3}	0.3590×10^{0}	0.2468×10^{-1}
a', g'		0.7501×10^{-3}	0.5412×10^{0}	0.5921×10^{-1}	0.1324×10^{-3}	0.3167×10^{0}	0.2497×10^{-1}
		(+28.2)	(−13.0)	(−2.4)	(+32.4)	(−11.8)	(+1.2)
a, g	0.20	0.1005×10^{-3}	0.6404×10^{-1}	0.8815×10^{-2}	0.9187×10^{-5}	0.3595×10^{-1}	0.2535×10^{-2}
a', g'		0.1129×10^{-3}	0.5729×10^{-1}	0.8689×10^{-2}	0.9182×10^{-5}	0.3128×10^{-1}	0.2498×10^{-2}
		(+12.34)	(−10.54)	(1.4)	(−0.1)	(−13.0)	(−1.5)
a, g	0.30	0.2638×10^{-5}	0.2486×10^{-2}	0.4966×10^{-3}	0.8600×10^{-7}	0.8177×10^{-3}	0.8494×10^{-4}
a', g'		0.8481×10^{-6}	0.2293×10^{-2}	0.4826×10^{-3}	0.5207×10^{-8}	0.7208×10^{-3}	0.8043×10^{-4}
		(−67.9)	(−7.8)	(−2.8)	(−93.9)	(−11.8)	(−5.3)

the values $a = 0.9$ fm^{-1} and $g^2 = 0.116\,67$ fm^{-3}, which were used in the calculations of preceding sections. The cross sections for the two sets of parameters are compared in Table II.

A larger value of the deuteron inverse range parameter a implies comparatively greater probability for large relative momenta and correspondingly reduced probabilities for low values of relative momenta in the deuteron wave function. As a result we find that at some places cross sections for one set of parameters are larger than those for the other set and vice versa, depending on the magnitude of the relative momentum that is important.

The main point which emerges from these comparisons is that the magnitude of the cross section, in the region where it is significant, does not depend critically on the choice of the set of parameters (from among the acceptable range indicated in the beginning of this section) used to describe the deuteron. This is mainly due to the fact that the binding energy of the deuteron, k_0^2, is very small compared to the square of inverse range, i.e., $k_0^2 \ll a^2$. As a result, in our model of the deuteron, k_0^2 (which is the same for all sets of parameters) governs the shape of the deuteron wave function [Eq. (3.3)] to a great extent.

IX. PAULI MECHANISM IN α-PARTICLE REACTIONS

The α particle is another among the most frequently used bound multinucleon projectiles in nuclear reactions. It is a tightly bound system and therefore, has large values of relative momenta available. The individual particle momenta for an α particle with center-of-mass momentum K_0 will therefore have a wide spread around the value $\frac{1}{4}K_0$ which is the average momentum of each of the four constituents in the α particle. In other words, in the Fourier analysis of the α-particle wave function into plane-wave products (in a manner analogous to the description of Sec. II) there will be a large preponderence of the low-

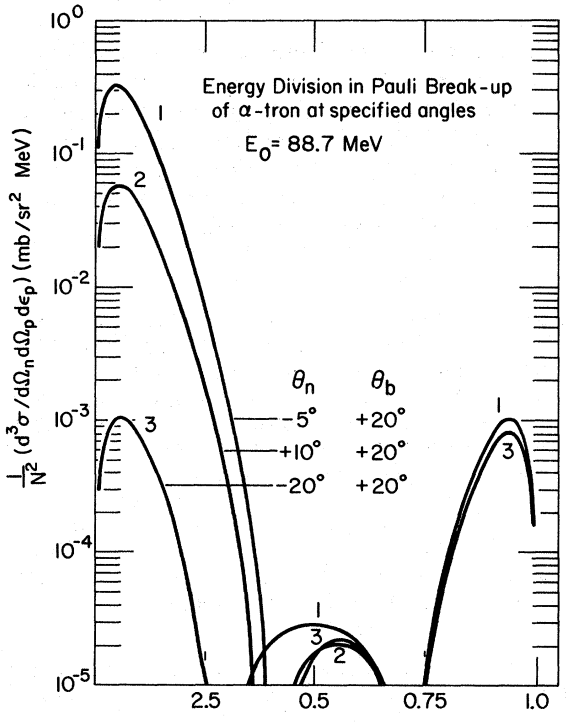

FIG. 8. Same as in Fig. 4 but for the case of α-tron (the artifically tightly bound deuteron). The main difference between α particle and the deuteron (apart from complexity of structure) is that the α particle is much more tightly bound. Therefore, the results in this figure suggest (comparing them with those of Fig. 4) that in α-particle reactions the Pauli mechanism also plays an important role.

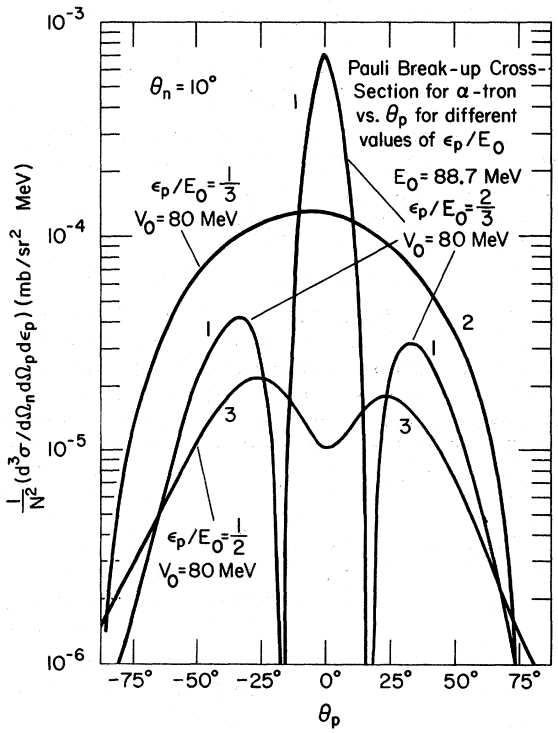

FIG. 9. Same as in Fig. 5 but now for the case of α-tron. The effect of the availability of large relative momenta in the α-tron wave function is completely offset by the fact that a greater transfer of energy from center-of-mass motion to relative motion is required to bring about the breakup of α-tron. As a result both the figures (5 and 9) show similar distributions and magnitudes.

momentum plane waves. Thus, one expects the Pauli mechanism to be very important in α-particle reactions.

However, the major difficulty in dealing with α-particle reactions is that the α-particle consists of four nucleons as compared to deuteron's two. Therefore, the problem of including the Pauli mechanism, even in the inert and infinitely heavy target model of Sec. IV, is a formidable one.

Nevertheless, one can perhaps mock up the effect of tight binding in α particle by considering an artificially tightly bound deuteron. One can imagine four nucleons of the α particles to be bound together by six binary bonds each with a strength $=\frac{1}{6}\epsilon_\alpha$, where ϵ_α is the binding energy of the α particle. We therefore suggest that the artificially tightly bound deuteron which we intend to use as a proxy for the α particle should have a binding energy $=\frac{1}{6}\epsilon_\alpha$ and a size comparable to the size of the α particle. We shall refer to this artificial deuteron as the α-tron. We use the same model for it as that for the deuteron but with the following parameters

$$a_\alpha = 1.4 \text{ fm}^{-1} \quad g_\alpha^2 = 0.428 \text{ fm}^{-3}. \tag{9.1}$$

These parameters correspond to a binding energy of 4.7 MeV and mean square radius $=8.5$ fm^2 which are consistent with the above suggestion.

The calculated results for Pauli breakup of ~89-MeV α-trons on ^{16}O are shown in Figs. 8 and 9 (cf. Figs. 4 and 5 for the deuteron). The Pauli mechanism now has to cause a greater transfer of energy from center-of-mass motion to relative motion in order to bring about the breakup. This completely offsets the effects of large relative momenta being available in α-tron. As a result there is marked similarity between the α-tron and the deuteron results. The only pronounced difference is the existence of relatively pronounced secondary maxima in $\epsilon_p/E_0=\frac{2}{3}$ curve in Fig. 9. This is a consequence of interference between the forward-peaked (T_1+T_2) terms on the one hand and the $PV_{np}^{\alpha}P$ term on the other (see Sec. VIII B). Since V_{np} is a much weaker potential than V_{np}^{α}, the secondary maxima are very weak in the case of the deuteron (<10^{-5} mb/sr^2 MeV).

If our simple model is adequate in simulating the main qualitative features of the α particle, then these results show that the Pauli mechanism plays an equally important role in the α-particle reactions.

X. CONCLUSIONS

In our calculations of deuteron breakup we have considered only one target nucleus, namely ^{16}O. However, we believe that the general features for the Pauli breakup will apply to other target nuclei as well, since they arise not from specific details of the ^{16}O nucleus, but from qualitative properties which it shares with other nuclei. This confidence is reinforced by the success of our general predictions made in Sec. III on the basis of variation of the binding energy of the deuteron with its center-of-mass momentum and with the density of nuclear matter through which it propagates. Of course, specific detailed differences among target nuclei are to be expected. They would seem to promise rewarding theoretical and experimental studies for the future.

Apart from the interesting features of energy and angular correlations, the quantity of greatest practical interest is the magnitude of the cross section, since it determines whether the process is of experimental interest at the presently available level of experimental precision. Unfortunately, in this calculation, as in most, the absolute magnitude of the cross sections is difficult to estimate reliably.

If one believes with us that our present assumptions are reasonable enough, then the strong dependence of the cross section on incident energy indicates that at lower energies[29] (~40–50 MeV) the process ought to be within the purview of current experimental techniques. In particular reactions leading to extremely asymmetric partitions of energy among breakup products are expected to have large cross sections, and therefore to be encouraging for an experimental test.

Finally, by considering Pauli breakup of an artificially tightly bound deuteron (referred to as the α-tron), we conclude that the Pauli mechanism plays an important role in α-particle reactions also.

APPENDIX A

After determining the normalization constant $C^2=ak_0(a+k_0)^3/\pi^2g^2=k_0(a+k_0)$ for our model deuteron of Sec. III, we transform to the coordinate representation and then obtain for the mean square radius the following expression which does not involve the parameter g:

$$\langle r^2\rangle = 1/2k_0^2+3/2ak_0+1/2a^2+2/(a+k_0)^2. \tag{A1}$$

This quartic equation can be shown[23] to have a unique positive solution for $1/2k_0^2<\langle r^2\rangle<5/4k_0^2$. The values of $\langle r^2\rangle$ used in various deuteron models all lie within this range. Thus, for all cases of interest, a simple computer program can be used to determine the unqiue positive root of Eq. (A1). Once a is known, the corresponding value of g can be easily obtained from Eq. (3.5) by substitut-

TABLE III. Choice of deuteron parameters, a and g. Values of $\langle r^2\rangle$, the mean square radius, and g^2, the potential strength parameter, for different values of the inverse range parameter a. The deuteron binding energy is the same in each case, i.e., 2.226 MeV.

a (fm^{-1})	$\langle r^2\rangle$ (fm^2)	g^2 (fm^{-3})	g^2/a^3	% deviation of g^2/a^3 from a mean value of 0.1530
0.9	18.70	0.116 77	0.1552	+1.438
1.0	17.62	0.153 69	0.1537	+0.457
1.1	16.75	0.197 62	0.1528	−0.131
1.2	16.04	0.249 19	0.1523	−0.457
1.3	15.45	0.308 98	0.1522	−0.523
1.4	14.95	0.377 62	0.1522	−0.523
1.5	14.53	0.455 71	0.1525	−0.327
1.6	14.16	0.543 85	0.1529	−0.065

ing for a and k_0. However, for the present purpose, we calculated the values of $\langle r^2\rangle$, g^2, and g^2/a^3 for several values of a. The results are shown in Table III. Notice that $\langle r^2\rangle$ does not depend strongly on a. Therefore, uncertainties in the value of $\langle r^2\rangle$ make it difficult to select a unique value of a. We picked $a = 0.9$ fm^{-1} for our calculations as this corresponds to a range of 1.1 fm for the neutron-proton interaction.

As a side remark, notice from Table III that all these sets of parameters which correspond to the same binding energy but somewhat different value of $\langle r^2\rangle$ satisfy an approximate condition $g^2/a^3 \simeq a$ dimensionless constant. This is exact analog of the well-known fact that on the basis of low-energy two-nucleon data it is difficult to distinguish between two local potentials with the same value of V_0R^2. Here V_0 and R stand for strength and the range of the potential.

APPENDIX B. PROOF OF COMPACTNESS OF THE KERNELS

For all three processes – breakup, elastic scattering, and stripping – the kernel of the integral equations is the same:

$$K = G_i \bar{V}_{np} G_c V_x W_i^\dagger , \tag{B1}$$

with the various operators given by equations in Sec. V A.

We want to show that K is a compact or Hilbert-Schmidt (H-S) kernel, i.e.,

$$\text{Trace } K^\dagger K < \infty \quad \text{or} \quad \text{trace } KK^\dagger < \infty . \tag{B2}$$

For this purpose we need the following theorems which are stated without proof. The interested reader is referred to standard texts.[30,31] These theorems are usually stated and proved for completely continuous (CC) operators which include the H-S integral operators as a subclass.[30]

Theorem 1. If A is a CC operator and B is bounded operator then both AB and BA are CC operators.

Theorem 2. If A and B are CC operators then $A + B$ is also a CC operator.

Returning to the task of proving that the kernel given in Eq. (B1) is compact, we use Theorem 1 to drop the wave operator $W_i^\dagger$ which is a bounded operator of norm 1. Thus we need consider only the kernel

$$K_1 = G_i \bar{V}_{np} G_c V_x . \tag{B3}$$

However, instead of K_1 we shall consider[32] a simpler but more singular kernel K_2, given below, so that a proof of the H-S property for K_2 will suffice as a proof of H-S property of K_1 and hence of K. We obtain K_2 by replacing both the Green's functions G_i and G_c by free Green's function G_0. We also relax some of the restrictions on potentials $\bar{V}_{np}$ and V_x, i.e., we replace $\bar{V}_{np}$ by V_{np} and replace $V_x = -QH_dP - PH_d$ by

$$V_{xa} = -H_d P - PH_d . \tag{B4}$$

Thus we define K_2 to be

$$K_2 = G_0 V_{np} G_0 V_{xa} . \tag{B5}$$

Using plane-wave states as a complete basis,

$$\text{Trace } K_2 K_2^\dagger = \int_{kK,k''K''} \langle \vec{k}\vec{K}|K_2|\vec{k}''\vec{K}''\rangle \langle \vec{k}''\vec{K}''|K_2^\dagger|\vec{k}\vec{K}\rangle$$
$$= \int_{kKk''K''} |\langle \vec{k}\vec{K}|K_2|\vec{k}''\vec{K}''\rangle|^2 . \tag{B6}$$

Notice that the operator P [Eq. (5.2)] allows δ function in either one particle coordinate or the other but not in both simultaneously. Therefore V_{xa} can have a δ function in individual particle coordinates separately. However, these δ functions will be taken care of by V_{np} which restricts the relative coordinate of the two particles. Therefore, there are no troublesome δ functions involved in the matrix elements of K_2. The proof of H-S property, therefore, involves only substitutions and finally, power counting to test the convergence of the integral.

Substituting Eq. (B5) for K_2 into Eq. (B6), and inserting another set of plane-wave states between

V_{xa} and G_0, we obtain

$$\text{Trace } K_2K_2^\dagger = \int_{kK,k''K''} \left| \frac{f(k)}{(E_0^- - E)} \int_{k'} \frac{f(k')}{(E_0^+ - E')} \langle \vec{k}'\vec{K} | V_{xa} | \vec{k}''\vec{K}'' \rangle \right|^2 . \tag{B7}$$

Here we have used $\langle \vec{k}\vec{K} | G_0 = \langle \vec{k}\vec{K} | (E_0^- - E)$; $E = \frac{1}{4}K^2 + k^2$ and $\langle \vec{k}\vec{K} | V_{np} | \vec{k}'\vec{K}' \rangle = V_{np}(k|k')\delta^3(\vec{K} - \vec{K}')$. Also $E' = \frac{1}{4}K^2 + k'^2$.

Substituting for V_{xa} from Eq. (B4), we get

$$M = \langle \vec{k}'\vec{K} | V_{xa} | \vec{k}''\vec{K}'' \rangle = -\langle \vec{k}'\vec{K} | P(E'' + V_{np}) + (E' + V_{np})P | \vec{k}''\vec{K}'' \rangle , \tag{B8}$$

where $E'' = \frac{1}{4}K''^2 + k''^2$. The most singular part of this matrix element is [after substitution for P from Eq. (7.4)]

$$M_s = E'E'' \langle \vec{k}'\vec{K} | P | \vec{k}''\vec{K}'' \rangle = -E'E'' | \delta^3(\vec{k}' - \vec{k}'' + \tfrac{1}{2}Q) \sum_\alpha \bar{\psi}_\alpha(\vec{k}'_-)\psi_\alpha(\vec{k} - \vec{k}''_+) + \delta^3(\vec{k}' - \vec{k}'' - \tfrac{1}{2}Q \sum_\beta \bar{\psi}_\beta(\vec{k}''_+)\psi_\beta(\vec{K} - \vec{k}''_-)| , \tag{B9}$$

where $\vec{k}''_\pm = \frac{1}{2}\vec{K}'' \pm \vec{k}''$ and $\vec{Q} = \vec{K} - \vec{K}''$.

The most singular contribution to the trace will be obtained when M_s is substituted for the matrix element of V_{xa} in Eq. (B7),

$$I_s = \int_{kK,k''K''} E''^2 \left| \frac{f(k)}{E_0^- - E} \left[\frac{f(\frac{1}{2}Q'' - k'')}{E_0^+ - E_1'} E_1' \sum_\alpha \bar{\psi}_\alpha(\vec{k}''_-)\psi_\alpha(\vec{K} - \vec{k}''_+) + \text{a similar term} \right] \right|^2 . \tag{B10}$$

Here E_1' is the value of E' when the δ function in Eq. (B9) is taken care of.

Using the fact that all nuclear bound-state wave functions die off at least exponentially and can diverge at the origin at most as r^{-1}, we could have set an upper bound for all of them to be $\psi_\alpha(k) < C/(k^2 + s^2)$, where C is an arbitrary large number and $s^2/2m$ is the separation energy of the last bound particle. Thus we set an upper limit to I_s

$$I_s < A \int_{kK,k''K''} E''^2 \left| \frac{f(k)}{E_0^- - E} \left[\frac{f(\frac{1}{2}Q'' - \vec{k}'')E_1'}{E_0^+ - E_1'} \frac{1}{s^2 + k''^2_-} \frac{1}{s^2 + (\vec{K} - \vec{k}''_+)^2} + \text{a similar term} \right] \right|^2 , \tag{B11}$$

where A is another arbitrarily large constant.

Counting the powers, since $f(k) = g/(k^2 + a^2)$, we have 16 powers of momenta in the denominator for a 12-dimensional integral. Hence the integral converges. Since I_s was the most singular contribution to Trace $K_2K_2^\dagger$, we therefore conclude that other contributions are also finite.

As a result

$$\text{Trace } K_2K_2^\dagger < \infty . \tag{B12}$$

Thus K_2 and hence K [Eq. (B1)] is a compact kernel.

APPENDIX C

Here we want to investigate the validity of the third approximation of Sec. VII A which replaced the scattering state $\langle \chi_{\vec{k}'}^- |$ by the plane-wave state $\langle \vec{k}' |$ in Eq. (7.3). With V_{np} given by 3.1 we get

$$\langle \chi_{\vec{k}'}^- | = \langle k' | + \langle k | C(k')f(k)/(k^2 - k'^2 - i\epsilon) , \tag{C1}$$

where

$$[C(k')]^{-1} = 1/f(k') - (\pi^2/a)f(k')(a^2 - k'^2 + 2iak') . \tag{C2}$$

Thus the correction term for $\langle \vec{k}'\vec{K}' | P | \phi_0\vec{K}_0^+ \rangle$, the first matrix element in Eq. (7.3), due to the scattered part of final state is

$$M_{1s} = \int \frac{f(k)C(k')}{k^2 - k'^2 - i\epsilon} \langle \vec{k}\vec{K}' | P | \phi_0\vec{K}_0^+ \rangle d^3k \sim f(k')C(k') \frac{\pi i}{2k'} k'^2 \int d\Omega_{k'_s} \langle \vec{k}'_s\vec{K}' | P | \phi_0\vec{K}_0^+ \rangle , \tag{C3}$$

where $\vec{k}'_s$ is such that $|\vec{k}'_s| = k'$.

The matrix element $\langle \vec{k}_s' \vec{K}' | P | \phi_0 \vec{K}_0^+ \rangle$ is strongly peaked in the forward direction (Sec. VIII B). Thus when $\vec{k}'$ also has proper alignment, i.e., in the region of large cross sections,

$$\int d\Omega_{k_s'} \langle \vec{k}_s' \vec{K}' | P | \phi_0 K_0^+ \rangle \sim \langle \vec{k}' \vec{K}' | P | \phi_0 K_0^+ \rangle . \tag{C4}$$

Thus in the region of large cross sections, the ratio of final-state scattering correction term to the term retained is (in magnitude)

$$A_s(k') = \tfrac{1}{2}\pi k' f(k') | C(k') | . \tag{C5}$$

$A_s(k')$ is a measure of the importance of scattering by V_{np} in the final state. $A_s(k')$ as a function of k' is plotted in Fig. 10. It is apparent from this figure that the contribution to Pauli breakup amplitude from the scattered part of the final state is at most a few percent of the contribution from the plane-wave part of the final state, and our approximation is correct to within a few percent.

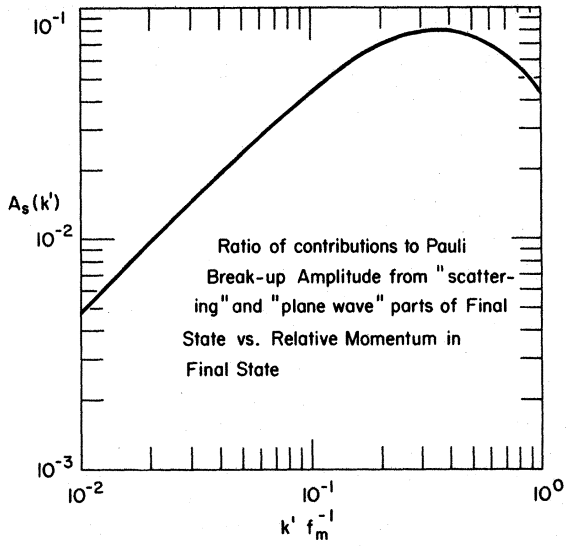

FIG. 10. The ratio of contribution to forward Pauli breakup amplitude from the "scattering part" of final state to the contribution from plane-wave part is plotted as a function of k', the magnitude of relative momentum in final state. The figure shows that the error involved in neglecting final-state distortions due to V_{np} is less than 10%.

APPENDIX D

Here we outline the approximate scheme used to evaluate $\langle \vec{k}' \vec{K}' | P V_{np} P | \phi_0 K_0^+ \rangle$, the fourth term in transition amplitude (7.11). We start with Eq. (7.7) and evaluate only the first term (denoted by T_{4a} in the following). After substituting for nuclear state sums, we make first the transformation $\vec{k} = \frac{1}{2}K_0^+ + \vec{q}$ and then $\vec{K} = 2(\vec{k} + \vec{k}_-' + \vec{B})$; $\vec{B} = (2\vec{k}_-' - \frac{1}{2}K_0^+)3$. The purpose of these transformations is to simplify the Gaussian exponents such that they will involve only the squares of new variables of integration. Thus

$$T_{4a} = -16 C_0^{12} \alpha_0^{-6} e^{-A_4/2\alpha_0^2} \int d^3q f(\vec{K}_0^+/2 + \vec{q}) e^{-q^2/\alpha_0^2} \int d^3k f(\vec{B} - \vec{k}) \phi_0(\vec{D} - \vec{k} - \vec{q}) e^{-3k^2/\alpha_0^2}$$
$$\times [1 + 2\alpha_0^{-2} \vec{k}_+' (2\vec{k} + \vec{l})] \{1 + 2\alpha_0^{-2} [q^2 - (\vec{k} - \vec{l})^2]\}, \tag{D1}$$

where

$$\vec{l} = (\vec{K}_0^+ - \vec{k}_-')/3, \quad \vec{D} = (\tfrac{1}{2}\vec{K}_0^+ + \vec{k}_-')/3, \quad A_4 = k_+'^2 + 3l^2 . \tag{D2}$$

At the high incident energies considered here ($K_0^+ > 4 f_m^{-1}$), $\frac{1}{4}K_0^{+2}$, B^2, and D^2 are much greater than α_0^2. Therefore the ϕ_0 and the f functions do not vary appreciably over the important range of integration determined by the Gaussian factors. We, therefore, expand the k integrand (leaving the Gaussian exponentials alone) in Taylor series about $k = 0$ up to second power and then carry out the k integration. Same approximation was used to perform the final q integration, with the result

$$T_{4a} = -f(\tfrac{1}{2}\vec{K}_0^+) f(\vec{B}) \phi_0(\vec{D}) e^{-A_4/2\alpha_0^2} F(\vec{k}', \vec{K}', \vec{K}_0^+) 16/3\sqrt{3} . \tag{D3}$$

Here the dimensionless factor F is given by

$$F = 3 - 2l^2/\alpha_0^2 + \vec{k}_+' \cdot \vec{l} \alpha_0^{-2} (\tfrac{26}{3} - 4l^2/\alpha_0^2) + 4(\epsilon_1 + C) f_1(B)/3 - 4(\epsilon_2 + C)\phi_1/3$$
$$+ 4(\epsilon_3 + 2C)\alpha_0^2 \phi_1 f_1(\tfrac{1}{2}K_0^+)/3 + (\tfrac{4}{3})(\epsilon_4 + C)\alpha_0^2 \{2.5\phi_2 + \phi_1^2 + 2D^2 \phi_1 [f_1(D) f_0(D) - 2\phi_2] - \vec{D} \cdot \vec{K}_0^+ \phi_2 f_1(\tfrac{1}{2}K_0^+)\}$$
$$+ [(D^2 - 3a^2) f_1^2(D) + (D^2 - 3k_0^2) f_0^2(D) + 4D^2 f_1(D) f_0(D) + (\tfrac{1}{4}K_0^{+2} - 3a^2) f_1^2(\tfrac{1}{2}K_0^+) + 2\vec{K}_0^+ \cdot \vec{D} \phi_1 f_1(\tfrac{1}{2}K_0^+)]$$
$$\times [2 \times 5\alpha_0^2 - l^2 + \vec{k}_+' \cdot \vec{l}(19 - 6l^2/\alpha_0^2)/3 + 2\alpha_0^2 (\epsilon_5 + C) f_1(B)/3 - 2\alpha_0^2 \phi_1 (\epsilon_4 + C)/3] . \tag{D4}$$

The new quantities in Eq. (D4) are defined below:

$$\epsilon_1 = (3\vec{I} + 7\vec{k}'_+)\cdot\vec{B}/3, \qquad \epsilon_2 = (3\vec{I} + 7\vec{k}'_+)\cdot\vec{D}/3, \qquad \epsilon_3 = (3\vec{I} + 13\vec{k}'_+)\cdot\vec{K}_0^+/3, \qquad \epsilon_4 = (3\vec{I} + 13\vec{k}'_+)\cdot\vec{D}/3,$$

$$\epsilon_5 = (3\vec{I} + 13\vec{k}'_+)\cdot\vec{B}/3, \qquad f_1(x) = 1/(x^2 + a^2), \qquad f_0(x) = 1/(k_0^2 + x^2), \qquad C = \vec{I}\cdot[\vec{k}'_+ \times (\vec{k}'_- \times \vec{K}_0^+)]/3\alpha_0^2,$$

$$\phi_1 = 1/(a^2 + D^2) + 1/(k_0^2 + D^2), \qquad \phi_2 = (a^2 + D^2)^{-2} + (k_0^2 + D^2)^{-2}.$$

---

*Research supported in part by the U. S. Atomic Energy Commission. Based in part on a report (University of Maryland, Physics Department Technical Report No. 72-044) submitted in August 1971 by B. L. Gambhir to the University of Maryland, College Park, in partial fulfillment of the requirements for the degree of Ph.D.

†Permanent address: Department of Physics and Astronomy, University of Maryland, College Park, Maryland 20742.

[1]J. Lindhard, M. Scharff, and H. E. Schiött, Kgl. Danske Videnskab. Selskab, Mat.-Fys. Medd. 33, No. 14, 6 (1963); A. Russek, Phys. Rev. 132, 246 (1963); W. Lichten, Phys. Rev. 164, 131 (1967).

[2]W. Brandt and R. Laubert, Phys. Rev. Letters 24, 1037 (1970), and earlier references therein.

[3]P. Swan, Proc. Roy. Soc. (London) 228, 10 (1955); Ann. Phys. (N.Y.) 48, 455 (1968).

[4]Y. C. Tang, E. Schmid, and K. Wildermuth, Phys. Rev. 131, 2631 (1963).

[5]S. Okai, S. C. Park. and K. Wildermuth, Z. Physik 184, 451 (1965).

[6]R. E. Brown and Y. C. Tang, Phys. Rev. 176, 1235 (1968).

[7]V. G. Neudatchin, V. L. Korotkikh, and V. P. Korennoy, Phys. Letters 34B, 581 (1971).

[8]W. F. Junkin and F. Villars, Ann. Phys. (N.Y.) 45, 93 (1967).

[9]D. J. Thouless, Nucl. Phys. 75, 128 (1966).

[10]G. Baumgärtner, Z. Physik 204, 17 (1967).

[11]R. C. Johnson and P. J. R. Soper, Phys. Rev. C 1, 976 (1970).

[12]B. L. Gambhir and J. J. Griffin, Bull. Am. Phys. Soc. 16, 580 (1971) gives a preliminary report.

[13]Y. Yamaguchi, Phys. Rev. 95, 1628 (1954).

[14]D. M. Redondo, W. M. Machado, and J. Osada, Nuovo Cimento 24, 688 (1962).

[15]H. Bando and A. Kuriyama, Progr. Theoret. Phys. Suppl. 41, 69 (1968).

[16]Here it is assumed, as in Sec. II, that a Fermi-sea description for infinite nuclear matter is adequate for the present purpose.

[17]The potential well that describes the infinite nuclear matter must have a well depth greater than $k_f^2/2M$ because the particle with momentum k_f is, by definition, bound. A deuteron with initial kinetic energy E_d on entering nuclear matter will therefore have kinetic energy $T_d > E_d + 2$. $k_f^2/2M > (2k_f^2/4M$ which corresponds to a center-of-mass momentum $K_0 > 2k_f$.

[18]B. L. Gambhir and J. J. Griffin, Bull. Am. Phys. Soc. 15, 504 (1970).

[19]This curve is for $k_1 = 1.3$ fm^{-1}; $\rho = 0.1484$ fm^{-3} which is comparable to central density in ^{16}O for which Pauli breakup cross sections are reported in this paper. For heavy nuclei the central density is equal to the equilibrium nuclear matter density, $\rho_N = 0.17$ fm^{-3}, which corresponds to $k_f = 1.36$ fm^{-1}. The curve for this value of k_f in Fig. 2 willl be in between curves II and III.

[20]B. L. Gambhir and J. J. Griffin, Phys. Rev. C 5, 1856 (1972). A more detailed account is given in University of Maryland Technical Report No. 72-044, 1971 (unpublished), B. Gambhir, Ph. D. thesis, University of Maryland, College Park, 1971 (unpublished).

[21]K. R. Greider and L. R. Dodd, Phys. Rev. 146, 671 (1966), describes the methods for introducing such potentials into the formal scattering problem.

[22]H. Goldstein, *Classical Mechanics* (Addison-Wesley, London, 1965), p. 92; I. E. McCarthy, *Introduction to Nuclear Theory* (Wiley, New York, 1968), pp. 352–63.

[23]M. L. Goldberger and K. M. Watson, *Collision Theory* (Wiley, New York, 1964), p. 92.

[24]K. W. Ford and A. M. Kaufman, Nuclear Data Table, U. S. Atomic Energy Commission (U. S. Government Printing Office, Washington, D. C., 1960), Part 4, p. 72.

[25]A. Bohr and B. R. Mottelson, *Nuclear Structure* (Benjamin, New York, 1969), Vol. I, pp. 213–240.

[26]These estimates differ significantly from those of Ref. 20 on account of improved averaging process.

[27]R. Serber, Phys. Rev. 72, 1008 (1947).

[28]A. C. Helmholst, E. M. McMillan, and D. C. Swell, Phys. Rev. 72, 1003 (1947).

[29]Calculated results for these low energies have not been reported because of the fact that our approximation $W_i^+|\phi_0 K_0\rangle \simeq N|\phi_0 K_0^+\rangle$ does not hold very well a these low energies. See Sec. VII A.

[30]I. Stakgold, *Boundary Value Problems of Mathematical Physics* (McMillan, New York, 1967), Vol. I., pp. 184–195.

[31]F. Reisz and B. S. Nagy, *Lêcons d'Analyse Fonctionelle* (Budapest Akademiai Kiado, 1952).

[32]An alert reader will realize that in effect we are using Theorem 2 above.